DEPARTMENT OF THE ARMY, ORDNANCE CORPS
RODMAN LABORATORY
WATERTOWN ARSENAL

Contract No. DA 19-020-505 ORD 451
with
Division of Sponsored Research, MIT

Final Report
1 July 1959

INVESTIGATION OF SOLIDIFICATION OF HIGH STRENGTH STEEL CASTINGS UNDER SIMULATED PRODUCTION CONDITIONS

by

Foundry Section
Metal Processing Division
Department of Metallurgy
Massachusetts Institute of Technology
Cambridge, Massachusetts

DEPARTMENT OF THE ARMY, ORDNANCE CORPS
RODMAN LABORATORY
WATERTOWN ARSENAL

Contract No. DA-19-020-505-ORD-4511

with

Division of Sponsored Research, M. I. T.

FINAL REPORT

1 July 1959

INVESTIGATION OF SOLIDIFICATION OF HIGH STRENGTH STEEL CASTINGS UNDER SIMULATED PRODUCTION CONDITIONS

by

Foundry Section
Metal Processing Division
Department of Metallurgy

Massachusetts Institute of Technology
Cambridge, Massachusetts

ABSTRACT

This report represents a summary of research conducted in the second year of what is expected to be a continuing research program on the effect of solidification variables on mechanical properties of high strength cast steel. A variety of different castings were poured and treated in various ways to study the effect of (1) thermal and nucleation variables on grain structure and microporosity, and (2) the effect of grain structure and microporosity on mechanical properties. A special microradiographic technique was developed to measure very small amounts of microporosity.

Cylinder castings (4" dia. x 4" high, top risered) were solidified under various thermal conditions to achieve varying degrees of directional solidification and different grain structures. Grain structure was also changed by (1) inserting a chill rod in the riser (resulting in grain refinement) and (2) vibrating the metal in the gating system (resulting in grain coarsening). Highest mechanical properties were in zones of columnar grains, where almost complete freedom from microporosity was obtained; maximum properties were 270,000 psi tensile strength, 27 percent elongation.

Plate castings (1/2" thick, 5" wide, varying lengths) were cast to study the effect of plate length and chilling on microporosity and mechanical properties of simulated production castings. It was shown the microporosity (much smaller than can be detected by ordinary inspection techniques) has an important influence on properties of these castings. Maximum properties in the plate castings were obtained in regions of minimum porosity and were 260,000 psi ultimate tensile strength with 40 percent reduction in area.

Step wedge and "flow-out" castings were also cast and examined. Results from the step wedge castings showed that extremely high mechanical properties could be obtained through at least a two inch section by adequate control of thermal gradients. Mechanical properties of flow-out castings (in regions of low porosity) were the order of 290,000 psi tensile strength, 30 percent reduction of area.

Major conclusions of this work are that (1) in the case of the high purity metal used in this investigation, heat treated to the 250,000—300,000 psi strength level, microporosity in very small quantities is extremely deleterious to mechanical properties, particularly elongation and reduction in area, and (2) optimum directional solidification (steep thermal gradients) is essential to achieve freedom from microporosity; in the case of steel these steep thermal gradients usually produce columnar grains, and so freedom from microporosity and high ductility is, in this work, associated with the columnar zone portion of the steel castings.

TABLE OF CONTENTS

LIST OF FIGURES

LIST OF TABLES

I. GENERAL INTRODUCTION

There is a growing awareness on the part of the Ordnance Department, and of other sections of the military, of the benefits to be gained when sound, reliable, steel castings of ultra-high strength become readily available. When cast steels with strengths the order of 300,000 psi (and with adequate ductility and impact strength for Ordnance applications) become obtainable, their advantages will include a higher strength-to-weight ratio than the best forged aluminum or magnesium alloys now obtainable or anticipated. Also, the time and cost of producing such castings will in most cases be less than for producing forgings or fabrications of comparable quality.

At present, steel castings are not commercially available which have tensile strengths the order of 300,000 psi (and which have adequate ductility and impact strengths in heavy sections). However, as shown in this report, it is completely feasible to produce such castings under carefully controlled laboratory conditions. Moreover, it appears certain that, when the basic variables affecting mechanical properties of steel castings are fully understood on a laboratory scale, it will be possible to develop completely practical techniques for producing these high quality steel castings on a commercial basis.

Many of the problems presently encountered in production of high strength steel castings relate to the solidification mechanism of the alloy; the problems include hot tearing, some surface defects, microsegregation, microporosity, and segregation of nonmetallics. Research in this investigation has been primarily concerned with a study of this solidification mechanism, under simulated production conditions, with the two-fold objectives of (1) gaining a fundamental understanding of the solidification variables which affect mechanical properties of high strength cast steels, and (2) applying this understanding toward development of techniques for producing stronger steel castings. This report is, in effect, a progress report of the second year of a continuing investigation at M. I. T., supported by the Ordnance Department through Rodman Laboratory, Watertown Arsenal. Work during the first year of the program concentrated primarily on a study of the effect of solidification mode on (1) microsegregation, (2) microshrinkage, (3) inclusion count and distribution. An important conclusion of that work was that microporosity (in castings which are apparently sound when examined by ordinary techniques) is an important factor limiting the mechanical properties of high strength cast steels.

Work during the second year of this research program, reported herein, has dealt more extensively with studies of (1) solidification variables which determine casting macrostructure; i.e., columnar or equiaxed grains, (2) susceptibility to microporosity of zones of castings with different macrostructures, (3) careful and extensive measurement of microporosity in steel castings, and (4) the effect of structure and microporosity on mechanical properties. A modified 4340 alloy, developed at Watertown Arsenal, was used throughout this study.

II. LITERATURE SURVEY

A previous report[1], describing work conducted on this program in fiscal 1957-1958, contained an extensive literature survey on the effect of solidification variables on mechanical properties of high strength cast steels. It is the purpose of the survey included below to expand on that previously presented, and particularly to describe previous researches which have a direct bearing on the investigation reported herein. Specifically, this survey deals with (1) the effect of casting grain structure on cast metals and (2) factors affecting, and techniques for altering, casting grain structure.

A. Casting Structure and its Effect on Mechanical Properties

While the mechanical properties of castings are usually (and reliably) isotropic, specialized solidification conditions can produce castings with properties that are quite different in different directions. Walther, Adams, and Taylor[2] investigated the casting "fiber" in aluminum alloys by performing mechanical tests on materials which solidified with wholly columnar macrostructures. Their work showed that when tensile bars were tested along the axis of a dendrite, tensile strength and ductility were many times greater than in bars tested transverse to the dendrites. It was concluded that the low properties transverse to the columnar grains (dendrites) were due to microporosity and brittle segregate that lined up between the grains during solidification.

Northcott[3] also found anisotropy in the case of copper castings which were solidified with elongated columnar grains. In this case, however, the mechanical properties were lowest when pulled along the direction of the axis of the columnar grains (in contrast to the case of aluminum); also, the best properties were obtained when the structure of the cast material was equiaxed. Tensile specimens oriented transverse to the columnar zone axis showed intermediate strengths. In this case it appears that porosity or segregate had little effect on mechanical properties, and the variation in properties with varying structures was due solely to crystallographic (or grain boundary strengthening) effects.

Variation of mechanical properties of cast steel with the type of structure has been investigated by Northcott[4] and by Reynolds and Preece.[5] Northcott found, in the course of an investigation to determine the effect of turbulence on solidification structures, that the mechanical properties of cast steel in the equiaxed zone were inferior to properties in the columnar zone. He attributed these lower mechanical properties to the increased amount of porosity at the center of the casting, although no evaluation of the amount of porosity was undertaken at the time. Reynolds and Preece found the difference in strength level between crystals in the equiaxed zone and crystals in the columnar zone to be very slight; of the order of 2,000 pounds per square inch. However, the ductility was markedly different. The percentage reduction in area for columnar zone material was 47 percent compared to 28 percent reduction in area for material tested in the equiaxed zone.

Reynolds and Preece[5] also related structure to degree of microporosity and found the equiaxed zone more prone to the occurrence of microporosity than the columnar zone. It appears that the high reductions in area they obtained in the columnar zone are due

to the low amount of microporosity in this region. This explanation agrees with findings of Jackson[28] who showed that the degree of ductility increases as the amount of microporosity decreases. It should be emphasized that the work cited above has been conducted on commercial grade steel (with strengths the order of 50,000 psi); "microporosity" considered was of a much grosser type than that dealt with in the present investigation.

The changes produced in the length of the columnar zone and the size of the grains in the equiaxed zone have been investigated from various standpoints, including the action of grain refining materials, convection effects, turbulence effects and pouring temperature. Cibula[6] investigated the effects of grain refining additions to aluminum alloys and showed that the length of the columnar zone and grain size of the equiaxed zone are both greatly reduced by the addition of grain refining materials. Gray[7] found that by inserting a chill rod in the riser of a top fed casting, the columnar zone was reduced. This result was attributed to effects arising from convection in the mold. However, in the case of aluminum alloys, Hucke, Flemings, Adams, and Taylor[8] have shown that under very steep thermal gradients increasing the degree of stirring increases the tendency to form columnar grains. Reynolds and Preece[5] established through the use of stearin wax that a high degree of convection can exist prior to solidification. Northcott[9] investigated the role of alloy elements and their effect on the length of the columnar zone. He was able to distinguish between elements which increase, decrease, or do not affect the length of the zone in copper base materials. However, an explanation of the effects of alloy elements has not been satisfactorily expounded.

Russian investigators have found some unusual changes in structure as a result of the presence of dissolved gas. Polin[10] found that by allowing steel to solidify under an atmosphere of hydrogen of 0.2 to 0.3 atmosphere, the grains were elongated and the grain size increased. A fine equiaxed structure resulted in ingots solidified under vacuum up to pouring temperatures of 1580°C. Eminger and Kinsky[11] found that considerable reduction in the length of the columnar zone occurred if the steel was cast by pouring through a vacuum. The reduction of the columnar zone was attributed to the breaking up of dendrites by the action of gas evolution.

B. Factors Affecting Formation of Columnar Zone in Steel Castings

The structure of the columnar zone and the details of its formation are of particular interest from a commercial viewpoint since this structure is commonly found in steel castings and since the mechanical properties of metal from the columnar zone are usually higher than the properties of the equiaxed zone. Requirements for the formation of this zone have been discussed by Chalmers,[12] Tiller and Rutter,[13] Walker,[14] and Hucke, Flemings, et al[15]. During solidification of an alloy, solute is rejected to the liquid by the growing solid. This rejection results in formation of a boundary layer in the liquid (immediately ahead of the growing solid) which is richer in solute than the bulk liquid composition. Formation of the boundary layer, its thickness, and factors which affect it have been discussed by Wagner[16]. An important result of solute rejection during solidification is that it depresses the temperature at which freezing begins (liquidus temperature) of metal in the boundary layer adjacent to the growing solid. Figure 1a shows this depression schematically as a function of position in the liquid metal.

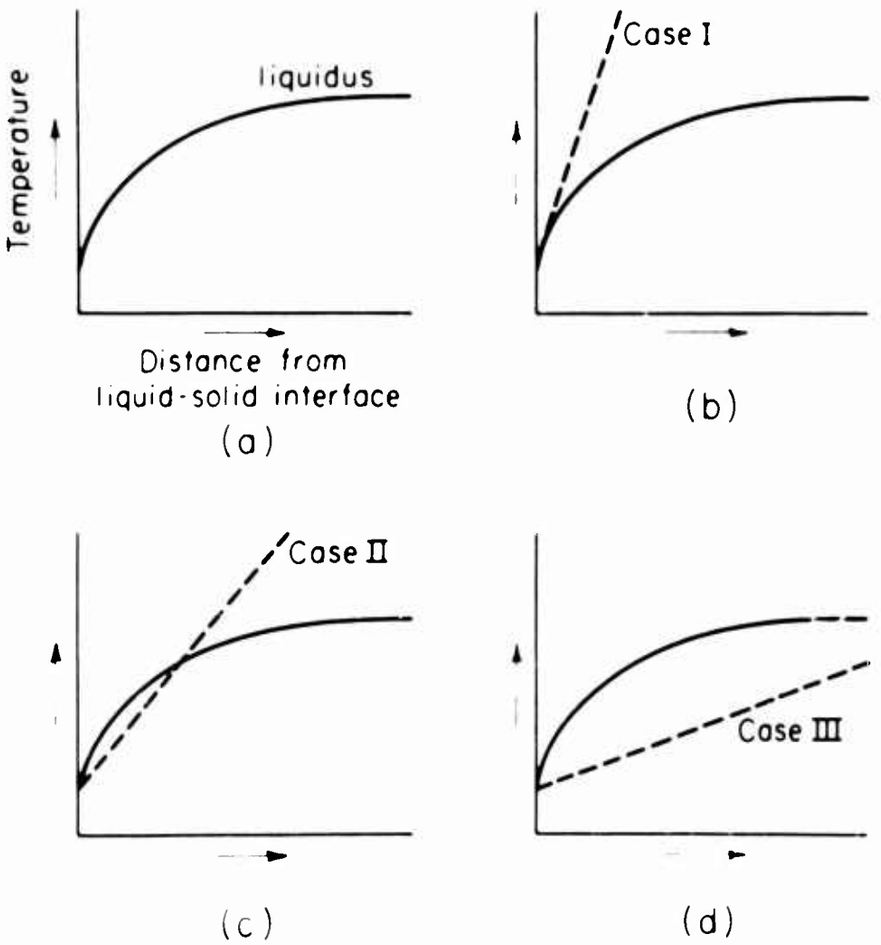

Figure 1 Conditions for the Formation of Cast Structures

(a) Depression of the liquidus temperature adjacent to the liquid-solid interface as a result of solute rejection during solidification.

(b) Steep temperature gradient resulting in plane front solidification

(c) Slight supercooling exists resulting in an unstable liquid-solid interface; dendrites are formed.

(d) Shallow temperature gradient resulting in the formation of an equiaxed region; nucleation occurs ahead of the interface.

It is possible to add to Figure 1a the actual temperature distribution (temperature gradients) existing in a solidifying casting; Figure 1b shows one possible case. In this example (Case I) temperature gradients are steep enough so that there is no point in advance of the interface that lies below the liquidus temperature at that point. In this case, solidification is "plane front"; dendrites do not form and the resulting casting is composed of large grains completely free of any microsegregation. This type of solidification can occur only with extremely pure metals or when special techniques are employed.[13]

If the actual temperature gradient in the casting is slightly less steep than the gradient of the liquidus temperature the situation shown in Figure 1c results (Case II). Here, at a point in advance of the interface, metal is below the temperature at which freezing can occur; the plane front of Case II is now unstable and a tendency exists for columnar grains (the columnar dendrites) to reach out into this "constitutionally supercooled liquid".[12] A discussion is given below of thermal and metallurgical factors which (1) promote columnar grain formation, or (2) lead to breakdown of columnar grains with consequent equiaxed grain solidification.

C. Factors Affecting Formation of Equiaxed Zone During Solidification

The formation of the equiaxed zone has historically been the least well understood of the grain structures found in castings and ingots. In one of the first systematic investigations of casting structures, Scheil[17] was unable to explain the formation of the central zone of equiaxed grains; he referred to it as abnormal nucleation since it did not agree with the laws of crystallization set forth by Tamman.[18] He recognized that nuclei must be present in the central portion of the casting, since grain refinement in this position was found to result from inoculation treatments, reduction in pouring temperature, and reduction of mold temperature. He also found a marked reduction in the length of the columnar zone and pouring temperature and mold preheat temperature were decreased. He offered two possible explanations for these observations: (1) that the nuclei were the result of movement of particles away from the growing solid and (2) that the grain refinement was related to what we now call "constitutional supercooling", the buildup of low melting point liquid around a solid, which inhibits further growth of the solid.

Scheil's first concept had, and has, merit for understanding certain nucleation phenomena. His idea was supported by his experiments with vibration which were found to refine the grain size. Genders[19] suggested this refinement results from the fracture of dendrites, although other explanations are possible, as proposed by Freedman and Wallace.[20, 21] Also, the work of Papapetrou[22] suggests secondary branches of dendrites may be attenuated at the backbone of dendrites and subsequently removed from it by re-solution.

Consideration of Scheil's second concept above leads immediately to reconsideration of the boundary layer theory outlined in earlier and detailed in Figure 1. Briefly, when the temperature gradients in a solidifying casting are relatively shallow, as shown in Figure 1d, then the degree of supercooling may be sufficient that nucleation occurs ahead of the interface and an equiaxed grain structure results. The amount of supercooling necessary to achieve this nucleation depends on the state of the metal bath; i.e. presence or absence of impurities, grain refiners, or the application of such external factors as vibrations.

D. Summary of Metallurgical and Thermal Factors Affecting Solidification Structure of Cast Metals

Based on the preceding discussion, and on pertinent references,[4, 8, 12, 13, 15] it is possible to delineate the factors which if wholly controlled in steel castings could result in castings of completely controlled grain structure. With reference to Figure 1, the following procedures will increase the length of columnar grain zone in steel castings:

(1) Increase the steepness of the temperature profile; i.e., steep temperature gradients.

(2) Decrease amount or availability of potential nuclei.

(3) Decrease steepness of the liquidus profile; this can be done experimentally by such techniques as stirring, slow solidification, or alteration of analysis.

Specifically, the following factors will promote the formation of a columnar zone; the reverse of those listed below will promote fine grain formation:

1. Mold materials of high thermal diffusivity.
2. Low thermal diffusivity of the cast metal (steel has a low value of thermal diffusivity).
3. High pouring temperature.
4. Absence of potential nuclei in the melt.
5. A value of the partition coefficient that is high (small separation of the liquidus and solidus lines).
6. Stirring at the liquid-solid interface.
7. Low solute concentration.
8. High liquid diffusion rate of the solute.

III. EXPERIMENTAL PROCEDURE

A. General

Several types of castings were designed and rigged so as to produce various structures, feeding conditions, and freezing rates. Each casting was subjected to the following program:

1. The macrostructure was examined by sectioning and etching with a neutral solution of copper ammonium chloride. (120 gms. copper ammonium chloride per 1000 cc of water).
2. The mechanical properties of heat treated samples from various locations were measured by tensile and impact testing.
3. A survey of the amount of microporosity existing at various locations was performed by thin section radiography; i. e., microradiography.

B. Foundry Data

1. Melting and Pouring Procedure

Melting was carried out in a magnesia-lined induction furnace of 300 pound capacity. Electrolytic iron, ferro-molybdenum and electrolytic nickel squares were placed in the furnace as charge materials. At meltdown, ferro-silicon containing approximately 50 percent silicon was added to the melt. The carbon was introduced at this point in the melting cycle in the form of a master alloy of high purity iron containing 4.2 percent carbon. Chromium was added in the form of ferro-chrome. The melt was heated to 3020°F and ferro-manganese charged. The melt was tapped at 3100°F into a preheated magnesia-lined ladle. A proprietary calcium-manganese-silicon deoxidizer was placed on the bottom of the ladle immediately before tapping. Four-tenths weight percent of deoxidizer was added. In addition, one-tenth weight percent aluminum was plunged into the ladle when two-thirds of the heat had been tapped. Temperatures during melting were measured with an optical pyrometer; ladle temperatures were measured with a platinum-platinum 13% rhodium immersion thermocouple.

2. Alloy Analysis

The alloy used throughout this investigation was one developed at Watertown Arsenal specifically as a high strength cast steel alloy. It conforms to the specifications for A. I. S. I. grade 4340.

3. Molding Materials

A sand composition listed in Table II was molded for all experiments in this work. When exothermic material was utilized, it was prepared by mixing Exomold "E", a proprietary composition, with seven to eight percent water. The mold was then baked overnight at 600°F to drive off the water.

TABLE I

Aim Analysis of A. I. S. I. 4340 Alloy

Element	Weight Percent
Carbon	0.40
Silicon	0.30
Manganese	0.80
Nickel	1.80
Chromium	0.80
Molybdenum	0.30
Phosphorous	less than 0.010
Sulfur	less than 0.010

TABLE II

Steel Sand Mixture

Number 80 Silica Sand	100 lbs.
Cereal	0.5 "
Dextrin	0.5 "
Western Bentonite	4.0 "
Water	3.2 "

TABLE III

Heat Treatment Schedule

Temperature	Time	Quench
2200°F	3 hours	Air cool to room temperature*
1750°F	3 hours	Air cool to room temperature**
1600°F	3 hours	Furnace cool to 1400°F
1400°F	2 hours	Oil quench
400°F	2 hours	Water quench
400°F	2 hours	Water quench

* Samples were generally cooled to a black heat and immediately placed in a furnace at 1750°F.

**Samples were shot-blasted after this treatment to remove scale.

C. Mechanical Testing

Test coupons were cut from the castings at various locations and heat treated according to the schedule in Table III.

Standard 0.347 inch diameter test specimens were prepared for tensile testing. Load versus elongation curves were recorded; from these curves, ultimate tensile strengths, and yield strengths at 0.1 percent and 0.2 percent offset were determined. The percent elongation and percent reduction in area were measured directly from the tensile test specimen. Standard Charpy bars were also prepared and tested at -40^{O}F.

D. Macrostructure Examination

Sections were taken from each test casting and etched with a solution of 120 grams of cupric amonium chloride dissolved in a liter of water. No elaborate surface preparation is necessary with the use of this etchant. The use of the neutral solution brings out the grain boundaries; addition of 50 cubic centimeters concentrated hydrochloric acid to 1000 cubic centimeters of neutral solution will reveal the dendrite arms.

E. Microradiography

The technique of microradiography consists in placing a thin sample in the beam of X-rays and collection of the transmitted image on a piece of photographic film. Generally, the photographic film is placed in direct contact with the sample so that a one-to-one correspondence with the sample is obtained. However, the sample may be removed some distance from the photographic emulsion, so that the image is enlarged directly. An article by Trillat[23] contains a review of the fundamental aspects of this technique and its value for many types of investigations. The more important factors as related to the study of microporosity are reviewed here.

Figure 2 points out the essential geometric conditions whereby microradiography is able to distinguish a second phase in a material. Consider a beam of X-rays of intensity I_0 falling on a sample of thickness x_1 containing a second phase of thickness x_2. The absorption coefficient of the homogeneous material is μ_1 and the absorption coefficnent of the second phase is μ_2. The ratio of the intensity of the transmitted ray through the homogeneous material, I_1, to the intensity of the ray transmitted through the second phase, I_2, is the photographic contrast and is given by:

$$\frac{I_2}{I_1} = \exp\left\{(\mu_1 - \mu_2)\, x_2\right\} \tag{1}$$

If the second phase is a microcavity, then μ_2 is equal to zero so that equation 1 reduces to:

$$\frac{I_2}{I_1} = \exp\left\{\mu_1 x_2\right\} \tag{2}$$

Therefore, the choice of radiation on the basis of absorption coefficient is not very important in the determination of amounts of microcavities. However, it is desirable from a practical

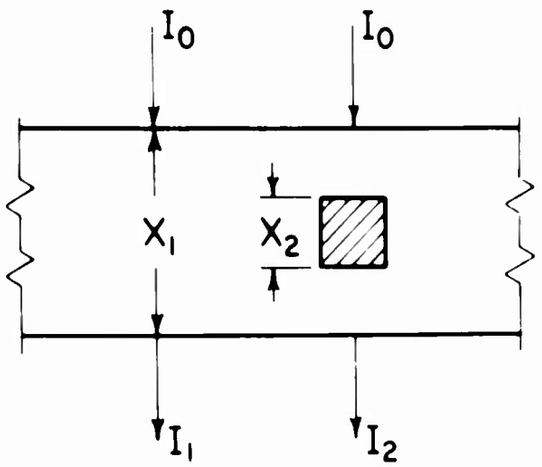

Figure 2 Geometric Conditions of Microradiography

standpoint to allow μ_1 to be as small as possible in order to reduce exposure time and the possibility of scatter.

In the identification of a second phase, radiation wave length is important to obtain qualitative and quantitative measurements. A plot of the linear absorption coefficient of a particular element shows a discontinuity at the absorption edge of the material. If a sample is X-rayed twice, once with radiation corresponding to a wave length where the absorption coefficient is high, and again with radiation where the absorption coefficient is low, then the sign of the difference between μ_1 and μ_2 is changed. That is, in the first case the second phase appears light and in the second case the second phase appears dark. With the aid of published values of absorption coefficients, positive identification can be made. Such information for inclusions found in steels has been published by Homes and Gouzou.[24]

The choice of photographic film becomes important when high magnifications are considered. Since the negatives may be enlarged up to 500 times, the grain of the film can obscure the desired results. Engstrom and Lindstrom[25] have discussed the suitability of various types of emulsions for microradiographic use. The best emulsions are Lipmann films or Eastman Kodak Spectroscopic Plates which have a resolving power of about 1,000 lines per millimeter.

Kodak High Resolution Plates have a resolving power of 500 lines per millimeter. Unfortunately, as the grain size is reduced to obtain higher resolution, the film speed is also reduced. This factor results in extremely long, impractical exposure times. When magnifications of the order of fifty times are required, films such as Kodak Contrast Process Ortho are desirable since they require relatively short exposure times.

Perhaps the chief drawback to the microradiographic technique is the difficulty of preparing suitable test pieces. It is necessary that the specimen be thin, of the order of 0.006 inches for precision work, have a good metallurgical polish on both sides, and parallel faces. Several methods have been suggested for preparation of these samples.[26, 27] One of the best appears to be that suggested by Sharpe.[28] He proposes that a sample holder be machined consisting of a thick plate with a large flat headed screw through it. The sample is mounted to the head of the screw with an adhesive, polished flat on one side, removed, remounted and polished flat to the desired thickness on the other side. The thick plate part of the holder permits easy handling and assures the final specimen is of uniform thickness.

Michael and Bever[26] prepared thin samples for autoradiography by mounting them in lucite and machining them on a lathe. This method has the advantage of speed; however, the final mechining operation is difficult since the specimens are fragile.

The requirements for samples for microradiographic inspection are:

1. They must have an excellent metallographic polish on both surfaces.
2. They must be thin, of the order of 0.006 inch.
3. They must have parallel surfaces.

In this work, the requirements were met by the following procedure:

1. The samples were cut as thin as possible on an abrasive cut-off wheel.
2. The samples were placed on a one-inch thick steel block whose surfaces had

been previously ground parallel. An epoxy resin of the composition listed in Table IV was poured over the samples and cured at 200°F for two hours.

TABLE IV

Epoxy Resin Mixture

Shell Epon Resin	10 ml
Hexahydrophthalic anhydride	11.5 ml
Pyridine	.04 ml

3. The block with the samples was placed on a horizontal grinding machine with a magnetic chuck and ground until the samples were about 0.010 inches thick.

4. Samples were removed from the block and mounted on a special holder with epoxy resin. The holder consists of a large screw of 1-1/4 inch diameter which was placed in the center of a steel block three inches square. After lightly polishing the surface to an excellent metallographic finish, the sample was removed and the process repeated on the unpolished surface to the final thickness.

5. The samples were radiographed on a General Electric X-ray machine of the type normally used for diffraction studies. Table V presents the important X-ray data.

TABLE V

X-Ray Data

Sample Thickness	.006 inch
Film to Source Distance	18 inches
Film	Contrast Process Ortho
X-Ray Tube	Copper Target
Voltage	40 Kilovolts
Current	7 milliamperes
Time	5 minutes

The amount of microporosity was evaluated by placing a grid on the radiograph and counting the number of squares in which micropores were found. The amount of microporosity was then determined as:

$$\text{Percent Microporosity} = \frac{\text{number of squares containing micropores x 100}}{\text{total number of squares}}$$

This method of rating microporosity results in a "percent microporosity" that is considerably magnified with respect to true volume percent. The magnification comes from the fact that the method, in effect, measures relative area of microporosity, but on a piece of finite thickness. The actual magnification probably depends somewhat on pore size as well as on experimental technique, but it does not appear unreasonable to expect the percent microporosity, as measured by this procedure is the order of 3 or 4 times the true volume percent.

IV. RESULTS AND DISCUSSION

A. Cylinder Castings

Effect of solidification variables on structure of cylinder castings was studied in castings that were 4" diameter by 4" high, top risered. Three castings were poured in each heat, all from a common gating system (Figure 3). Various techniques were employed to modify the structure of these cylinders, including (1) chill in the riser, (2) vibrated chill in the riser, (3) vibrating steel box in the ingate, (4) unvibrated steel box in the ingate, and (5) bottom chill. Table VI lists the heats poured and the techniques employed to modify casting structure. In each heat, one casting was poured with no treatment as a "standard".

TABLE VI

Cylinder Casting Treatment

Heat Number	Casting Number	Design Variable
A	1	3/4 inch diameter steel rod, 2 inches long with an air vibrator placed in the top of the riser.
	2	3/4 inch diameter steel rod, 2 inches long placed in the riser.
	3	standard gating system
B	1	2" x 2" x 4" steel box placed in the ingate with an air vibrator attached to the box.
	2	2" x 2" x 4" steel box placed in the ingate.
	3	standard gating system
C	1	3/4 inch diameter steel rod, 2 inches long placed in the top of the riser.
	2	3-inch diameter, 2-inch high cylindrical steel chill placed on the bottom surface of the casting.
	3	standard gating system

All heats were poured at a temperature of 2850^{0}F

Macrostructures of the test castings were examined by sectioning and etching vertical sections. Mechanical properties were determined by cutting test bars from locations shown in Figure 4. Microporosity ratings were determined by point counting microradiographs. Results of mechanical property evaluations, structure determinations and microporosity surveys are tabulated in Table VII and shown in Figures 5 through 7. Figure 5 reveals the marked refinement in grain size of the central zone of a casting when a chill rod is inserted in the riser. The addition of a vibrator produced no additional structure refinement above the change noted with the rod alone. Consideration of the causes of this refinement leads to the conclusion that such refinement is the result of nuclei formation in the region of

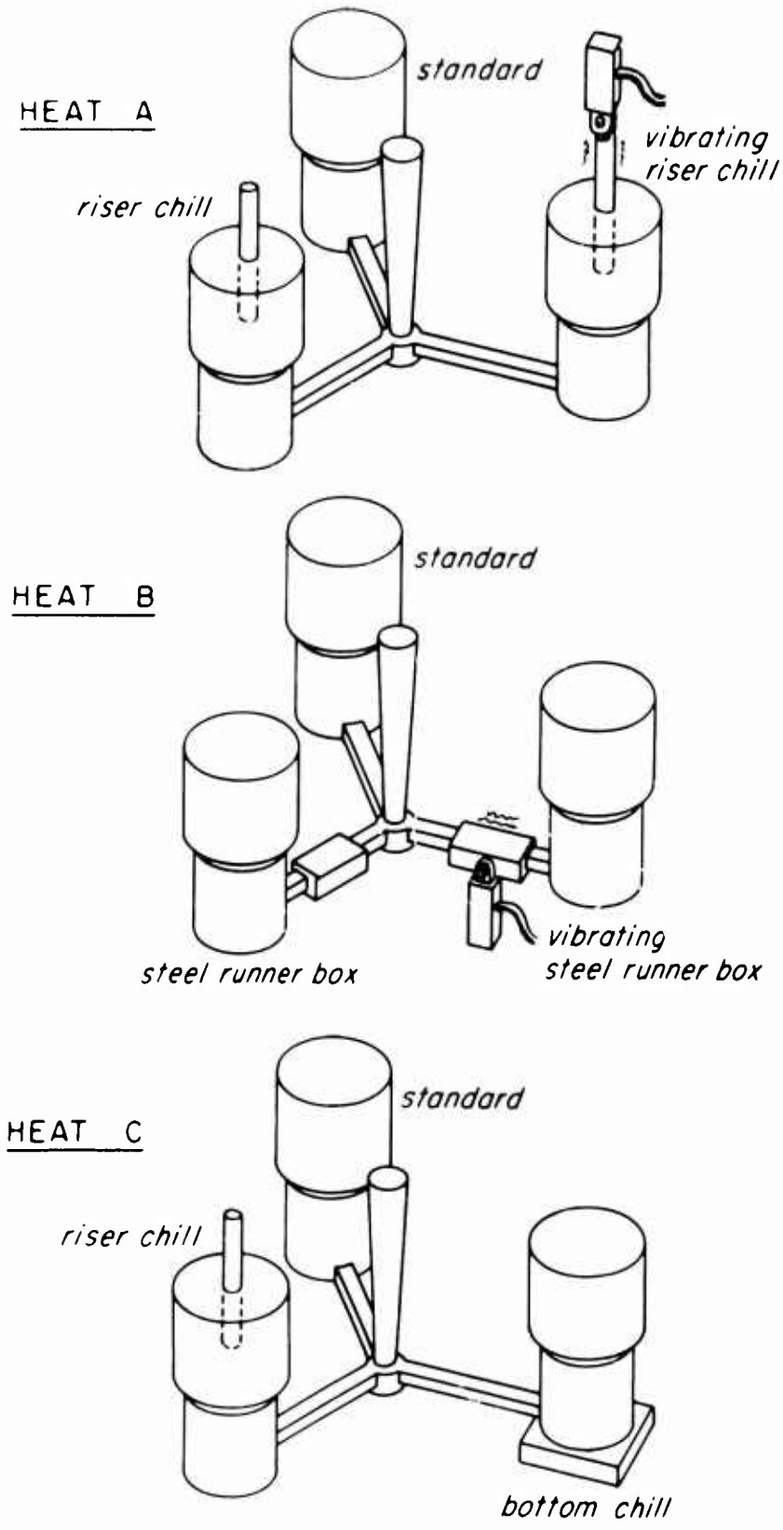

Figure 3 Gating Arrangement for Cylinder Castings

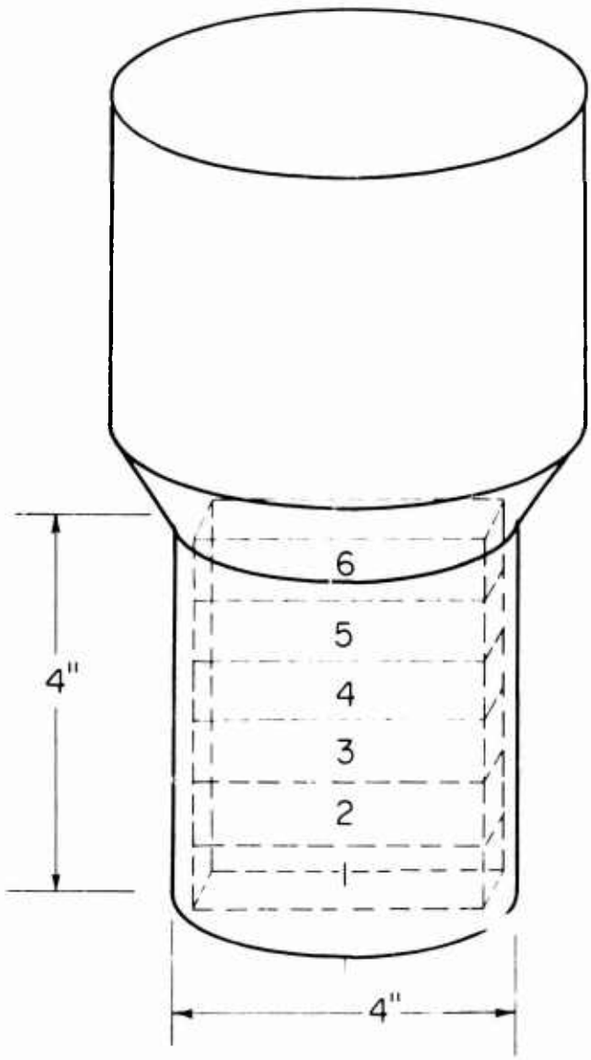

Figure 4 Cylinder Casting Design Showing Test Bar Locations

TABLE VII

Mechanical Properties of Cylinder Castings

No. *	Treatment	Structure	Loc. **	Y. S. 0.2% Offset lbs/in^2	Tensile Strength	Elong. %	Reduction in area %
A-1	vibrated chill rod in riser	fine grain size in the center zone	2	203,000	253,000	2.9	4.9
			4	204,000	255,000	3.6	6.0
			6	205,000	225,000	1.4	2.2
A-2	chill rod in the riser	fine grain size in the center zone	2	219,000	260,000	4.3	8.2
			4	215,400	259,900	4.0	5.5
			5	215,000	253,600	5.0	8.8
A-3	comparison standard	coarse grains in the center zone	1	211,000	258,000	4.3	10.9
			2	215,000	258,000	4.3	9.3
			3	215,000	254,000	2.1	4.4
			4	217,000	258,800	3.0	4.2
			5	219,500	264,600	5.0	5.6
			6	216,000	252,000	2.0	2.6
B-1	vibrated chill box in the gate	very coarse grains	1	211,000	265,000	3.6	3.8
			3	208,000	250,000	1.4	1.6
			5	209,000	263,000	4.3	7.1
			T	215,000	274,000	2.9	5.5
B-2	chill box in the gate	same as A-3	2	211,000	266,000	4.3	7.6
			4	217,000	264,000	3.6	6.6
			6	204,000	252,000	2.9	4.4
			T	206,250	260,000	3.6	9.3
B-3	comparison standard	same as A-3	2	207,000	264,000	5.0	6.6
			4	206,000	263,000	2.9	3.3
			T	211,000	268,000	2.9	4.9
C-1	chill rod in the riser	fine grain size in the center zone	1	228,500	277,500	7.9	16.1
			3	225,000	271,500	7.1	13.0
			5	224,000	267,500	4.3	5.5
C-2	chill on the bottom	columnar zone on the bottom region	1	218,000	270,000	10.7	27.0
			3	219,500	271,000	6.4	13.0
			5	224,000	272,000	3.6	5.5
			T	232,700	281,000	4.0	5.5
C-3	comparison standard	same as A-3	3	218,000	272,500	5.0	7.1
			5	223,500	273,000	4.3	6.0

Impact Data - Charpy Test

Casting	Location	Ft lbs (-40° F)	Casting	Location	Ft-lbs (-40° F)
A-1	1	8.3	B-3	1	11.7
	3	7.2		2	11.7
	5	10.9		3	7.2
A-2	1	10.9	C-1	2	8.2
	3	7.0		4	10.0
A-3	1	6.3		6	6.5
	2	10.3	C-2	3	6.3
B-1	2	11.2		4	6.7
	4	10.0		6	6.2
	6	11.3	C-3	2	5.2
B-2	1	11.4		4	5.5
	3	10.5		6	4.9
	5	11.8			

TABLE VII - Contd.

Microporosity Surve on Cylinder Castings

Casting*	Location**	Porosity (Percent)	Reduction in Area (Percent)
A-1	2	.90	4.9
	4	.91	6.0
	6	1.28	2.2
B-1	2	.51	3.8
	6	2.12	7.1
B-2	1	.70	7.6
	3	.67	6.6
	5	.81	4.4
C-1	1	.84	16.1
	2	.90	13.0
C-2	1	.38	27.0
	3	.53	13.0
	6	.13	5.5
C-3	1	1.17	
	2	1.34	7.1
	6	1.00	6.0

Chemical Analysis:

Heat	Element (weight percent)							
	C	Si	Mn	Cr	Ni	Mo	P	S
A	.37	.31	.87	.80	1.88	.25	.010	.008
B	.40	.40	.82	.85	1.77	.25	.007	.015
C	.41	.30	.69	.79	1.91	.24	.008	.012

* Letter refers to the heat, number to casting. All castings in a single heat were cast in the same mold.

** Number refers to Figure 4. The letter "T" indicates a bar cut from the casting transverse to the other bars from a region at the outside of the cylinder.

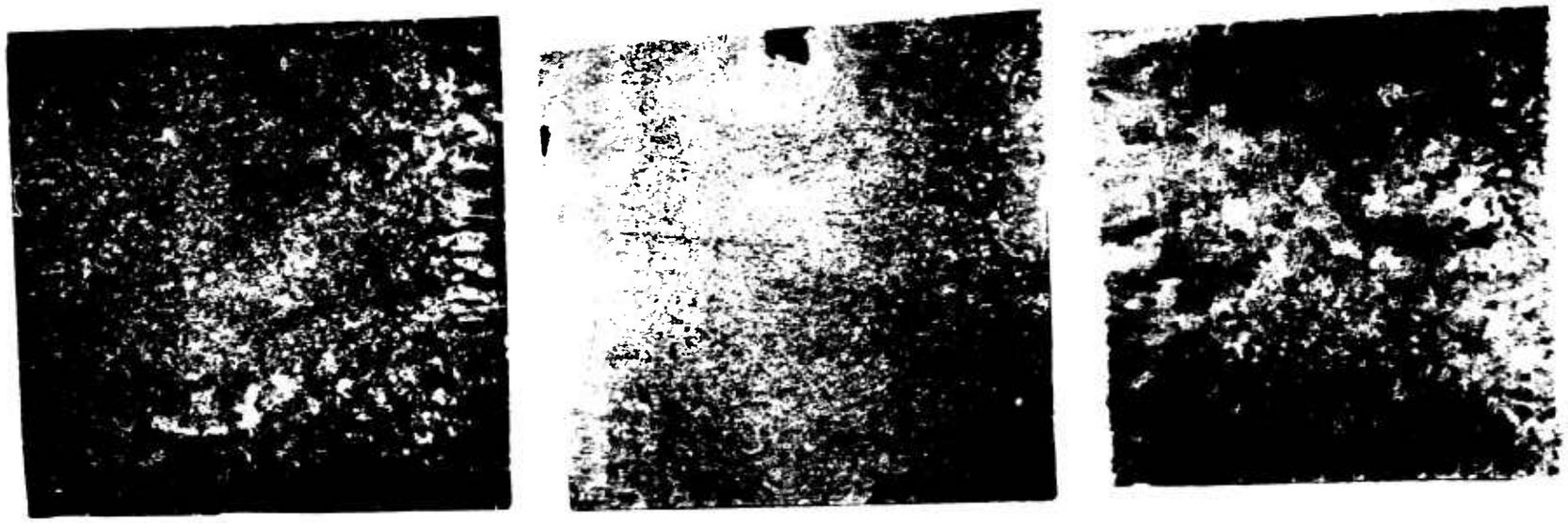

Casting A-1
Vibrated Chill Rod in the Riser

Casting A-2
Chill Rod in the Riser

Casting A-3
Standard Comparison

Figure 5 Macrostructures of Cylinder Castings, Heat A
(0.7 magnification, vertical section of the casting with the riser removed)

Casting B-1
Vibrated Chill
Box in the Gate

Casting B-2
Chill Box
in the Gate

Casting B-3
Standard
Comparison

Figure 6 Macrostructures of Cylinder Castings, Heat B
(0.5 magnification, vertical section of one-quarter of the casting)

Figure 7 Macrostructure of Cylinder Castings, Heat C
(Casting C-2, Chill on Bottom, 0.5X, vertical section of one-quarter of the castina)

the chill rod and the subsequent settling of these nuclei under the influence of gravity. This mechanism is discussed in more detail in a later section.

Agitation of the liquid steel immediately prior to entering the mold cavity results in grain corsening. This "denucleating" effect is illustrated by casting B-1 whose structure is presented in Figure 6. The columnar zone of this casting is extremely coarse and grains in the center portion of the casting are the largest grains found in any of the experimental castings. Large grains of this sort are characteristic of high pouring temperatures and/or slow cooling rates. Since the grain size of the two other castings poured in the same mold do not exhibit such coarsening, it must be concluded that the grain coarsening is the result of the addition of vibration.

The survey of mechanical properties reveals that yield strength and tensile strength are not affected by small amounts of microporosity. Any slight changes in strengths from heat to heat appear to result from small variation in carbon content. However, there is a marked effect of microporosity on ductility (reduction of area). Low amounts of microporosity result in high values of ductility. For example, a test bar from a casting in the region of a chill where the porosity value is 0.38 percent shows 27 percent reduction in area, whereas a sample from another location in the same casting where the porosity level is 1.34 percent, reduction in area is only 5.5 percent. These values are taken from the test casting C-2, a bottom chilled casting. The chill, by increasing thermal gradients, enhanced feeding at the bottom of the casting. Grain refinement (by insertion of a chill rod in the riser) apparently reduced porosity somewhat (0.90 percent compared to 1.00 to 1.30 percent in the comparison casting); however, this reduction in porosity was not sufficient to effect a significant improvement in ductility.

B. Plate Casting Experiments

A series of plate castings of varying lengths were poured; the plates were one-half inch thick, five inches wide, end risered (Figure 8). Plates were cast of five, three, and one inch lengths. One series of the plates were chilled at the end opposite the riser whereas a second comparison series was cast unchilled. Two separate heats of these plates (Heats D and E) were cast.

As a result of careful examination of the amount of microporosity present along the lengths of the plates (by the microradiographic technique described), and correlation of this porosity with location in the plate and with the chemical properties, the graphs of Figures 9 through 12 were prepared. These results are also presented in Table VIII. Major conclusions to be gained from these data are (1) a definite correlation exists between microporosity and reduction in area in the plate castings—relatively large amounts of microporosity are associated with low reduction of area, and (2) tensile and yield strengths are relatively unaffected by microporosity (in amounts studied).

Figure 12 averages the microporosity data from all heats and shows how amount of porosity depends on plate location and on whether or not the plate is chilled. It is important to note that all plates examined in this work were apparently sound when examined by ordinary X-ray techniques (to 2% definition).

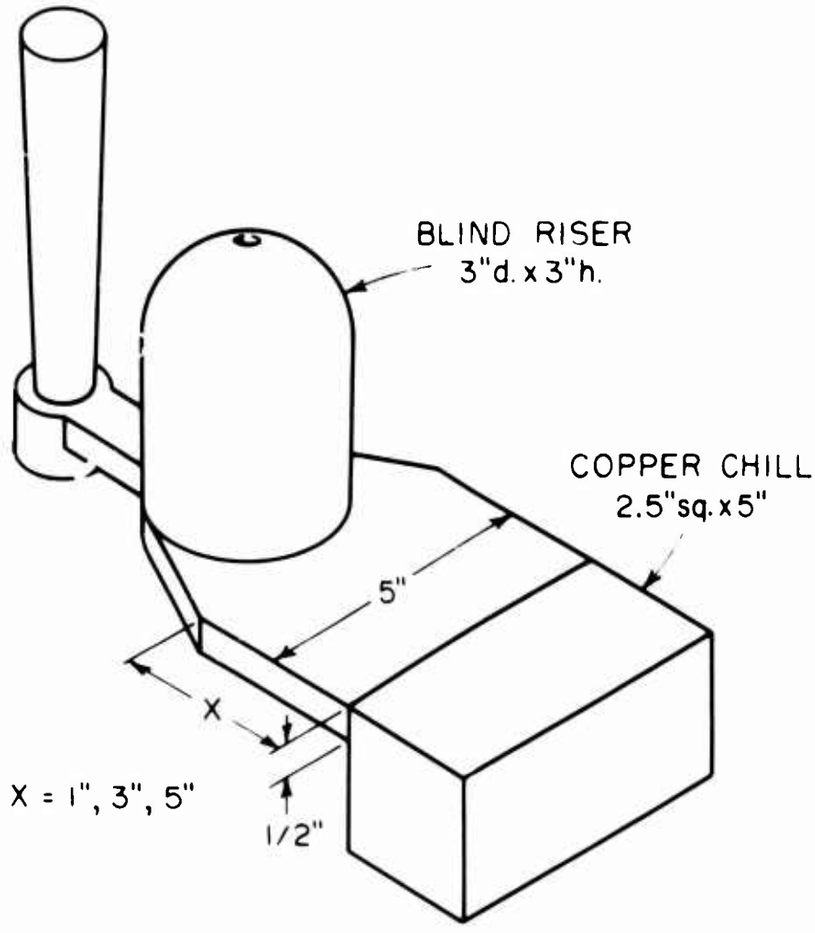

Figure 8 Plate Casting Design, Heat D and E

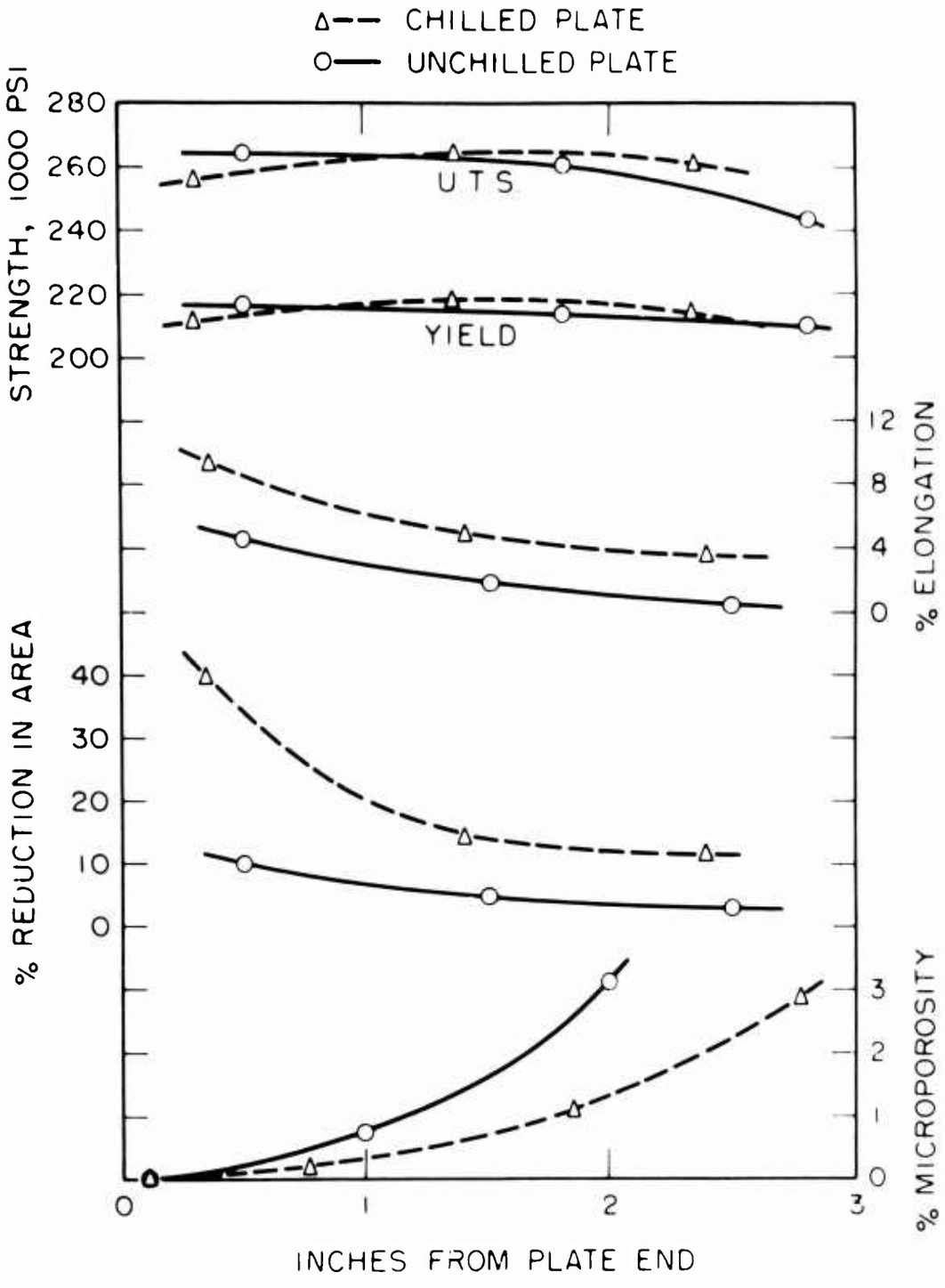

Figure 9 Summary of Tensile Test Data for 3 inch Plates, Heat D

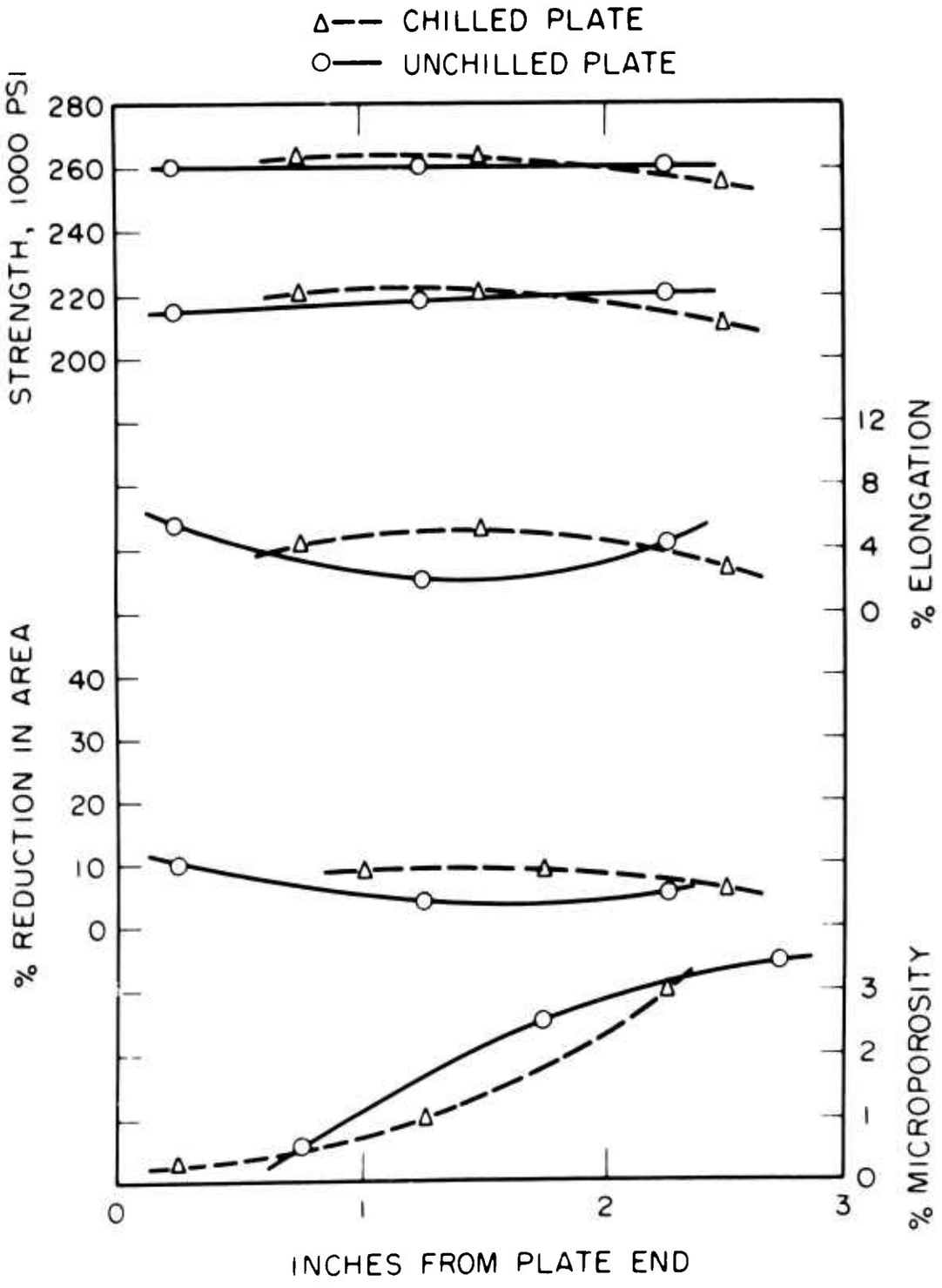

Figure 10 Summary of Tensile Test Data for 3 inch Plates, Heat E

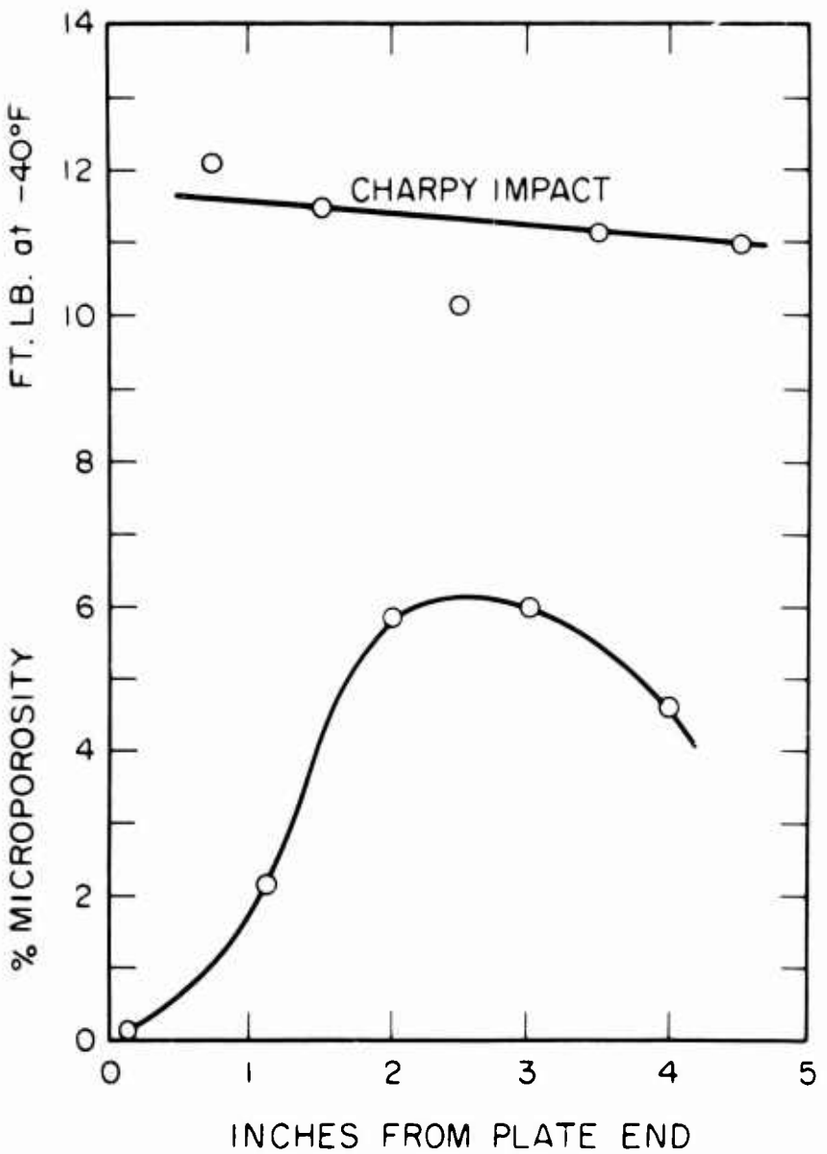

Figure 11 Summary of Charpy Impact Tests and Microporosity Data, Heat D

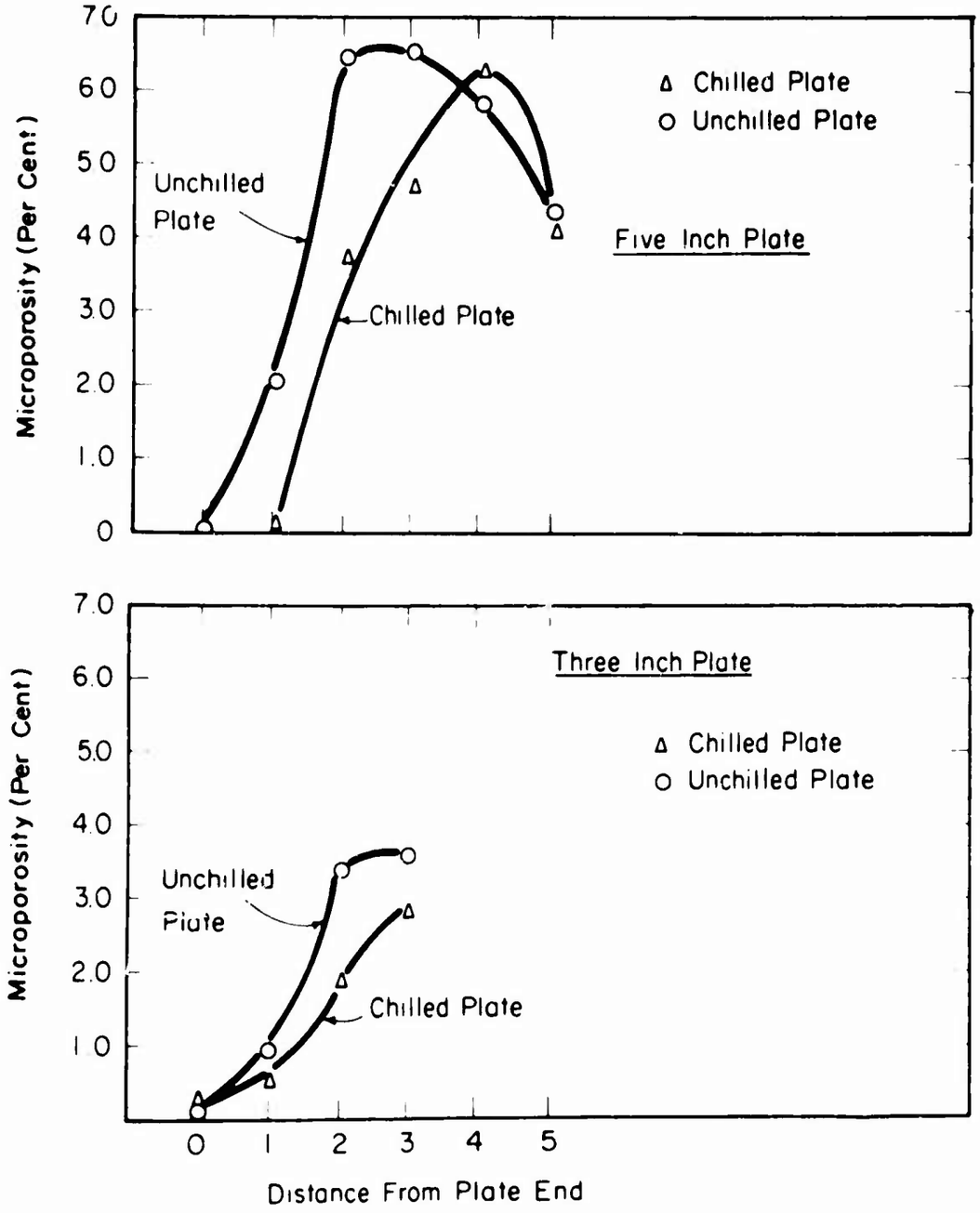

Figure 12 Microporisity Survey in Plate Castings (each point represents an average of data from two to four different castings)

TABLE VIII

Properties of Plate Castings

	Description	Plate Length inches	Location*	Y. S. 0.2% offset lbs/in^2	U. T. S. lbs/in^2	Elong. Percent	Reduction in area Percent	Percent Micro-porosity
	unchilled	1	0.5	216,000	262,000	5.7	15.6	0.90
	chilled	1	0.5	216,000	264,000	7.9	27.0	0.10
	unchilled	3	0.5	218,000	266,500	5.0	10.9	0.00
	"	3	1.5	216,000	262,000	2.1	5.5	0.71
	"	3	2.5	211,000	246,000	0.7	3.8	3.22
Heat	chilled	3	0.5	211,000	257,500	9 3	38.9	0.14
D	"	3	1.5	216,000	264,500	5 0	14.0	1.05
	"	3	2.5	215,000	262,000	3.6	11.9	2.89
	unchilled	5	0.5	216,000	265,000	2.1	3.8	1.05
	"	5	1.5	--	--	--	--	6.35
	"	5	2.5	213,000	242,000	0.7	3.3	3.54
	"	5	3.5	214,000	261,000	3.6	6.0	6.94
	"	5	4.5	216,000	258,000	1.4	4.4	4.33
	unchilled	1	0.5	217,000	265,750	6.4	11.4	0.16
	chilled	1	0.5	212,500	262,000	6.4	17.6	0.29
	unchilled	3	0.5	213,000	262,500	5.7	10.3	0.58
	"	3	1.5	214,000	260,000	2.1	3.3	2.57
	"	3	2.5	215,000	261,000	4.3	4.4	3.60
Heat	chilled	3	0.5	217,000	264,500	4.3	8.7	0.21
E	"	3	1.5	216,000	263,500	5.0	8.2	0.91
	"	3	2.5	209,000	254,500	2.9	6.0	2.75
	unchilled	5	0.5	215,500	259,000	2.1	3.8	0.16
	"	5	1.5	213,500	226,500	2.1	3.8	3.45
	"	5	2.5	212,250	220,000	2.9	3.3	8.12
	"	5	3.5	211,500	211,500	0.0	0.0	10.50
	"	5	4.5	207,000	257,000	4.8	4.4	4.70
	chilled	5	0.5	214,000	265,000	5.7	7.6	0.21
	"	5	1.5	215,500	267,500	5.0	8.7	3.76
	"	5	2.5	215,000	266,000	2.9	3.8	2.74
	"	5	3.5	215,000	260,000	4.3	5.5	6.53

Chemical Analyses:

	Element (Weight Percent)							
	C	Si	Mn	Cr	Ni	Mo	P	S
Heat D	.38	.32	.72	.87	1.87	.25	.007	.009
Heat E	.40	.25	.85	.80	1.81	.26	.013	.008

* Distance from plate end - inches.

Microporosity Survey in Plate Castings*

Plate	Length		Distance from Plate End 1"	2"	3"	4"	5"
unchilled	1	0.68					
chilled	1	0.25					
unchilled	3	0.11	.97	3.46	3.60*		
chilled	3	0.21	.52	1.90	2.89*		
unchilled	5	0.04	2.04	6.47	6.53	5.89	4.33*
chilled	5		0.11	3.73	4.77	6.39	4.20

*All numbers except those with asterisks represent averages from two to four different plates.

TABLE VIII - Contd.

Impact Data

Heat	Description	Plate Length	Location	Ft-lbs
D	unchilled	1	0.5	10.3
E	unchilled	1	0.5	7.3
E	chilled	1	0.5	10.5
D	unchilled	3	0.5	7.5
		3	1.5	9.2
		3	2.5	7.3
D	chilled	5	0.5	12.6
			1.5	11.5
			2.5	10.1
			3.5	11.1
			4.5	11.0
E	unchilled	5	0.5	8.2
		5	1.5	6.4
		5	2.5	10.1
		5	3.5	7.2
		5	4.5	9.1
E	chilled	5	0.5	11.5
			1.5	7.6
			2.5	8.5
			3.5	7.2
			4.5	8.6

TABLE IX

Step Wedge Casting Treatments

		Mold Surface Treatment	
Heat Number	Casting Number	Top Surface	Bottom Surface
F	1	Green sand	Green sand
	2	Green sand	Copper chill
G	1	One-inch thickness exothermic material	Sand
	2	One-inch thickness exothermic material	Copper chill

All castings were poured at 2850^{O}F

Figures 9 and 10 show the relationship between mechanical properties, plate location, and microporosity for plates 3 inches long, and for two different heats. In Heat D (Figure 9) reductions in area as high as 40 percent was obtained when microporosity was essentially absent. High ductilities were not obtained in Heat E (Figure 10) probably because of the high phosphorous content (.013 percent); mechanical property data from Heat E are generally poor and are not included in later summary tabulation of the effect of microporosity on mechanical properties (e.g., Figure 19).

Mechanical property data for the 5-inch long plate are similar to those obtained for the 3-inch plates. Data for two plates, one chilled and one unchilled (Heat E) are given in Table VIII. Data for an unchilled plate (Heat D) are plotted in Figure 9 and given in Table VIII. Impact test data for the plates, somewhat surprisingly, show little correlation with microporosity. These data, for the 1, 3, and 5-inch plates are given in Table VIII. Data for the low phosphorous heat (Heat D) are plotted in Figure 11 versus plate location.

In Figure 12, a summary is given of the percent microporosity obtained in the three and five-inch plates (chilled and unchilled). It should be borne in mind that "percent microporosity" used herein refers to percent microporosity as determined by the special microradiographic technique employed. This "percent microporosity" is a greatly magnified quantity with respect to true volume percent. Figure 12 clearly illustrates that it is extremely difficult to feed a steel casting to complete soundness, and that such soundness is obtained only very near a chill or casting edge. Amount of microporosity obtained is dependent on degree of feeding and hence on thermal gradient; this microporosity therefore increases sharply with increasing distance from the plate end (or chill), and may or may not fall off slightly near a riser.

In summary, a conclusion may be made that (1) steel castings produced without extreme control of solidification possess substantial microporosity that is not detected by ordinary inspection techniques, and (2) the microporosity has an important effect on mechanical properties, particularly reduction in area.

C. Step Wedge Castings

A series of step wedge castings were prepared to investigate the influence of solidification rate and casting section size on formation of the columnar zone. Table IX summarizes the treatments employed to alter the freezing rates; Figure 13 illustrates design of the casting.

Castings produced in this series of experiments reveal the effect of section size and freezing rate on the structure and mechanical properties. Table X lists observations in regard to structure and properties while the macrostructures observed are illustrated in Figure 14.

Figure 14 shows that columnar grains may be grown throughout the entire thickness of a two-inch section provided a mold material, such as copper, of very high thermal diffusivity is employed. In this casting, exothermic material was placed on the cope surface of the casting to prevent solidification from occurring from this surface. The exothermic material burns at a temperature which is approximately the freezing point of the steel.

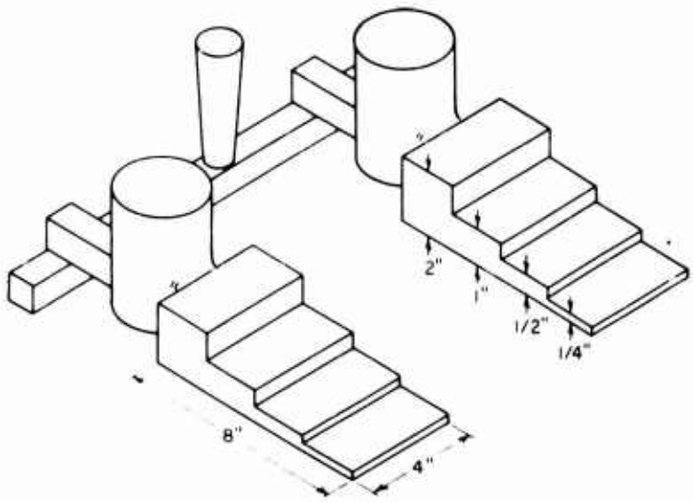

Figure 13 Step Wedge Casting Design, Heats F and G

TABLE X

Properties of Step Wedge Castings

Heat	Mold Surface cope	Mold Surface drag	Section Thick. inches	Structure Description	Y. S. 0.2% Offset lbs/in^2	T. S.[2] lbs/in^2	Elong. %	Reduction in area Percent
D	sand	sand	0.5	coarse columnar	211,000	262,500	3.6	13.0
	sand	sand	1.0	coarse columnar	205,000	265,000	2.9	7.6
	sand	copper	1.0	fine columnar	225,000	270,000	4.3	17.6
E	exo-thermic	sand	0.5	coarse columnar	201,000	260,000	5.7	13.5
	"	"	1	" "	205,500	265,000	2.9	4.4
	"	"	2B*	" "	208,000	270,000	4.3	6.0
	"	"	2M*	equiaxed	--	202,700[1]	0	0
	"	chill	0.5	fine columnar	217,000	266,000	10.0	35.4
	"	"	1	" "	209,000	257,000[1]	0	0
	"	"	2B*	" "	205,500	268,000	9.3	24.6
	"	"	2M*	" "	212,000	269,000	9.3	27.5
	"	"	2T*	" "	209,000	261,000	6.4	27.0

Chemical Analysis:

	Element (Weight Percent) C	Si	Mn	Cr	Ni	Mo	P	S
Heat F	.40	.31	.99	.97	2.27	.27	.009	.011
Heat G	.40	.28	1.01	.80	2.03	.24	.005	.012

[1]Broke in the threads.

*Letter refers to location in two-inch section B = bottom, M = middle, T = top

Microporosity Survey:	Percent (Percent)	Reduction in Area (Percent)
coarse columnar (sand)	1.60	4.4
fine columnar (chill)	.00	24.6

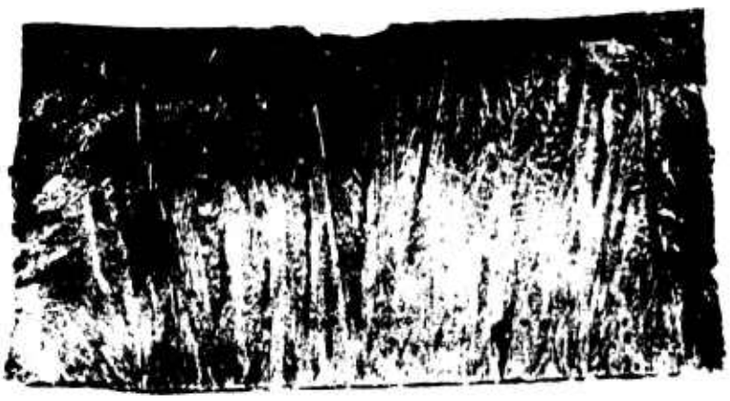

A. Exothermic Top Surface
Copper Bottom Surface

B. Exothermic Top Surface
Sand Bottom Surface

Figure 14 Macrostructures of Step Wedge Castings

C: Exothermic Top Surface
Copper Bottom Surface

D: Exothermic Top Surface
Sand Bottom Surface

E: Sand Top Surface
Copper Bottom Surface

F: Sand Top Surface
Sand Bottom Surface

Figure 14 (Continued) (One Inch Sections), Heats F and G

Since no heat is transferred to this surface, all solidification in these castings occurred from the bottom surface. When metal is cast against a sand surface, as is the case with the companion casting made in the same mold, thermal gradients are not very steep. Therefore, the columnar zone ceases to propagate after a time and the coarse-grained equiaxed region shown in Figure 14b is formed. These coarse grains are characteristic of the slow cooling rate prevailing in this part of the casting. When the castings are prepared without the exothermic material, solidification occurs from both surfaces. The columnar grains formed in contact with the chill copper surface grow at a faster rate than the grains formed in contact with the sand surface. This fact is evidenced by the displacement of the line at which both solidification fronts meet. With a sand cope and copper drag, the grains growing from the copper surface meet along a line three-quarters of the distance from the bottom surface of the casting.

Measurements of the amount of microporosity in the columnar region near a chill and the equiaxed zone indicate that the equiaxed zone contains appreciable amounts of microporosity, whereas the columnar zone is relatively free from this defect. Results of tensile testing show that the ductility in the vicinity of a chill is extremely good for this alloy steel heat-treated to this high strength level.

D. Vibration Experiments

Possible changes in the macrostructure of cast steel as a result of vibration during solidification were investigated by casting two block-like castings (3 1/2" x 3" x 2 1/4"), top risered, in a single mold. One casting contained a prong of steel, 1/2 inch in diameter and extending into the bottom of casting for a distance of one-half inch and vibrated at 3600 cycles per second with an amplitude of .050 inches. A similar unvibrated prong was inserted in the control casting. Two such heats, heat H and heat I were poured.

Heat H was poured at a temperature of 2840^{O}F. Upon examination of the macrostructure, no change was noted between the vibrated and unvibrated casting. In an effort to increase the columnar zone region, chills were applied to the sides of the casting in Heat I and the pouring temperature was increased to 2950^{O}F. Again no change was observed in the cast macrostructure. Examination of the microstructure at several locations of both castings revealed no change.

A survey of the mechanical properties of these castings is presented in Table XI. No marked changes are revealed. One possibility that may influence results of this experiment is the inadvertant vibration of the control casting by transmission of vibrations through the gating system. Results of this part of the investigation must be considered to be preliminary. The extremely good mechanical properties of these exceptionally sound castings leave open further avenues of research.

E. Flow-Out Casting Experiments

The effect of a flowing stream on the solidification of steel was investigated by the arrangement shown in Figure 15. Metal flowed through a one inch square channel for a distance of four inches across a water cooled, copper chill. Four castings were poured in a

TABLE XI

Properties of U. S. Rated and Unvibrated Castings

Heat	Description	Location*	Y. S. 0.2% Offset lbs/in^2	U. T. S. lbs/in^2	Elong. %	R. A. (Percent)
H	vibrated	1	208,000	258,000	10.0	35.4
	"	2	208,000	265,200	7.0	20.5
		3	205,000	268,400	8.0	19.2
H	unvibrated	1	207,000	265,600	10.0	34.0
	"	2	206,100	268,200	8.0	18.4
	"	3	204,000	262,800	8.0	14.7
I	vibrated	2	197,000	249,200	10.0	28.8
	"	1	196,900	247,900	10.0	37.5
I	unvibrated	1	200,000	251,000	11.0	36.8
		2	198,000	250,200	9.0	32.7

Chemical Analyses:	C	Mn	Si	Ni	Cr	Mo	P	S
Heat H	.37	1.06	.27	1.82	.82	.251	.011	.015
Heat I	.37	.91	.26	1.79	.81	.246	.011	.014

* Distance in inches from bottom of casting.

single mold. Various static layers of metal from zero to one inch were created between the flowing stream and the chill (Figure 15). A tapered section at the end of the runner acted as a control to keep the mold cavity full during the process.

The macrostructures of these castings (Figure 16) reveal a fine columnar zone in contact with the chill. At the top section of the casting there is a coarse equiaxed region. The coarseness of this region is characteristic of a slow cooling rate resulting from heating of the mold cavity prior to cessation of flow. Apparently only a small region in contact with the chill solidified while the stream was flowing. The remainder of the casting solidified in a static manner since the cubical basin at the end of the runner had become full. Approximately sixty pounds of metal flowed through each channel before flow ceased. Results of these experiments must be considered preliminary to future work. It is hoped to modify the procedure to obtain a longer flow time and thereby solidify a greater part of the casting while flow is occurring.

Tensile tests of these castings (Table XII) reveal the superiority of material tested in the columnar region over the material tested from the region of the coarse equiaxed zone. The steep thermal gradients which led to the formation of the columnar zone enhanced feeding conditions. Mold preheating (by the flowing metal stream) produced slow cooling conditions in the last region to solidify, giving rise to a coarse equiaxed zone containing large amounts of microporosity. The material tested from the static comparison piece, whose structure is essentially columnar, possesses properties equal to the high properties attained in material which is tested from the vicinity of a chill of the flow out castings. The high strengths associated with all of these test samples, save one which is the result of an imperfection present in the test bar, are the result of a slightly higher carbon content of this

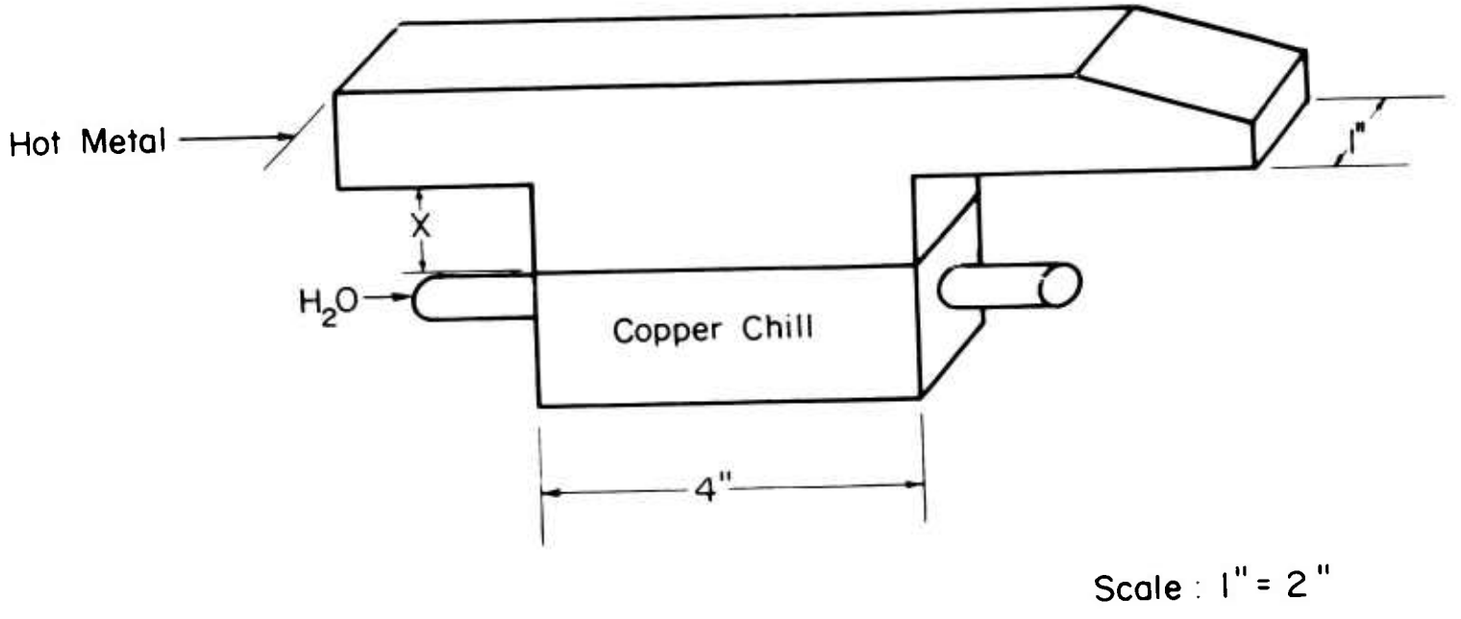

Figure 15 Flow-Out Casting Design, Heat J

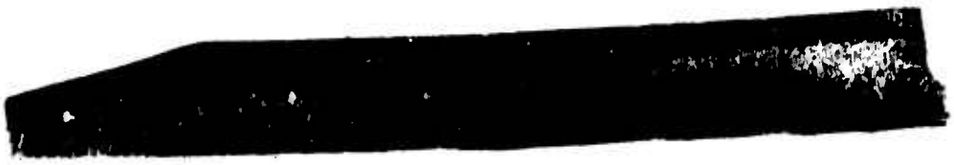

A: Static Cast Comparison

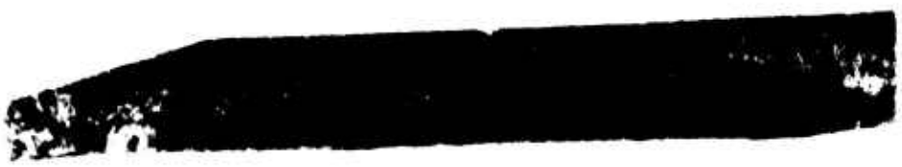

B: Zero Inch Static Layer

C: 1/4 Inch Static Layer

D: 1/2 Inch Static Layer

E: 1 Inch Static Layer

Figure 16 Macrostructures of Flow-Out Castings (.75 magnifications), Heat J

TABLE XII

Properties of Flow Out Castings

Casting*	Structure	Y. S. 0.2% Offset lbs/in^2	Tensile Strength lbs/in^2	Elong. Percent	Reduction in area Percent
0	columnar	222,200	284,500	10.0	30.3
1/4	equiaxed	--	--	0	0
1/4	columnar	219,500	294,000	7.9	24.1
1/2	equiaxed	215,500	224,000	0.7	1.1
1/2	columnar	220,000	288,500	8.6	28.9
1	top of columnar	217,500	280,000	6.4	18.1
1	bottom of columnar	218,750	280,000	7.9	28.4
static comparison	middle of casting fine equiaxed	224,500	291,000	10.0	29.8

Chemical Analysis:

	Element							
	C	Si	Mn	Cr	Ni	Mo	P	S
Heat J	.43	.33	.84	.83	1.91	.25	.007	.009

*Refers to the thickness of static layer.

Structure	Percent Porosity	Reduction in Area (Percent)
columnar	0.27	28.9
columnar-equiaxed interface	0.23	18.1
equiaxed	1.32	1.1

heat, 0.43 percent, than the carbon content of other heats, which is 0.40 to 0.38 percent carbon. The correlation of microporosity measured in several of the samples with the ductility reveals that samples containing large amounts of microporosity have poor ductility. The columnar zone is least prone to the occurrence of microporosity, whereas the equiaxed zone possesses a large amount of porosity.

F. Macrostructure Changes as a Result of Casting Treatment

The macrostructures presented in Figures 5 through 7 illustrate the profound changes in the cast structure of steel which can be obtained by alteration of solidification conditions (independent of metal chemistry and pouring temperature). The origin of these structures can be explained by consideration of (1) factors which promote formation of a columnar zone in castings and (2) factors which result in the breakdown of the columnar zone to form equiaxed crystals. These factors have been discussed in detail in the section

on "Literature Survey".

Castings A-1, A-2, and A-3 (see Figure 5) reveal the effect of a chill rod inserted in the riser of the casting. The addition of a chill rod produced substantial grain refinement in the casting. The addition of a vibrator to the rod produced no apparent effect above that of the chill rod alone. Considerations of the cause of this refinement, lead to the conclusion that refinement is the result of production of nuclei in the vicinity of the chill and the subsequent settling of these nuclei under the influence of gravity.

Calculations presented in the appendix, based on Stokes Law, prove that if spheres of the order of one millimeter or greater in diameter are formed, they will settle to the bottom of the casting within 100 seconds. Since the solidification time of the casting is greater than 600 seconds, this mechanism is entirely probable. In addition to the possibility of nuclei formation mentioned above, the chill effect of the rod from the standpoint of removal of superheat must be considered. If the chill removes superheat quickly it should produce much the same cast structure as would result from a reduction of pouring temperature. A calculation of the effect of the rod on superheat is presented below.

Calculation of the Effect of Chill Rod on Superheat

If the chill rod is assumed to be heated to its melting point by the superheat present in the liquid metal, then the heat effect, ΔH^S is given by:

$$\Delta H^S = \frac{V_r \rho_s}{M} \int_{T_o}^{t_m} CpdT \qquad (1)$$

where:

$\int_{T_o}^{t_m} CpdT$ = the heat required to raise one mole to its melting point and is equal to 14,150 calories for pure iron. This quantity includes the heat of solid to solid transformations.

V_r = the volume of the chill rod

ρ_s = the density of iron

M = the molecular weight of iron

The heat effect, $\Delta H'$, which is the heat removed from the liquid metal is

$$\Delta H' = \frac{V_c \rho_s}{M} Cp' \Delta T \qquad (2)$$

where:

C_p = the specific heat of the liquid, equal to 10 cal/mole for iron

T = the change in temperature

V_c = the volume of the casting

Since

$$\Delta H^S = \Delta H' \qquad (3)$$

then the equation for the change in superheat is given by:

$$\Delta T = \frac{14,150}{Cp} \frac{V_r}{V_c} \tag{4}$$

The calculation shows that such a chill rod can remove approximately one hundred centigrade degrees of superheat. However, the assumptions in this calculation are that the rod is heated entirely to its melting point and that none of the heat extracted by the rod is heat of fusion of the steel. Such is not the experimental case. The calculation is made to show the maximum effect this rod can exert. The rod was not uniformly heated to its melting point; indeed the upper part just approached a red heat. Also, a large amount of the liquid in contact with the rod froze immediately. This fact was observed in one heat where the rod was removed shortly after pouring. That the rod did not fuse to the casting, shows that it was not melted, so it could not exert an effect greater than that of being heated to its melting point.

Additional evidence can be cited to support the hypothesis that gravity plays an important role as a result of examination of some other castings. When a chill of more than twice the surface area than the rod surface area is placed at the bottom of a casting, as in the case shown in Figure 7, then grain refinement of the equiaxed zone does not occur, but the columnar zone is increased in length in the region of the chill. In another experiment, a chill rod of the same sort employed in this experiment, was placed in the casting at the bottom. No grain refinement was found to occur. Therefore, it may be concluded that grain refinement with a chill rod must be employed in conjunction with some mechanism for transporting the nuclei from the vicinity of the rod.

The structures observed in the step wedge castings and plate castings are typical of structures that are encountered under these test conditions. Steep temperature gradients, as in the case when a copper surface is placed in the mold cavity, result in the formation of a columnar zone. With a sand surface, the rate of growth and temperature gradients are decreased so that the possibility of degeneration of the columnar zone is increased. Observations presented in Figure 14 prove this hypothesis. Solidification in a flowing stream promotes the formation of a columnar zone by two mechanisms. First, new metal is continually arriving as the solidification interface so that thermal gradients are high. Second, any nuclei that form ahead of the interface are removed by the flowing stream.

G. Relationship of Structure to the Occurrence of Microporosity and the Effect on Mechanical Properties

The experimental results obtained in this study reveal that the mechanical properties of steel castings (as measured in a tensile test) are markedly dependent on the as-cast macrostructure of the test material. Material tested in the region which is fine-grained columnar is far superior to material tested in the region of the casting which is composed of equiaxed grains. In all castings produced, the incidence of microporosity was much higher in the equiaxed zone of the castings than in the columnar region.

Consideration of the causes of microporosity leads to the conclusion that the incidence of such porosity is lower in the columnar zone than in the equiaxed zone of castings because of the conditions which lead to the formation of the columnar zone; these conditions

are the same as those leading to good directional solidification and feeding (Figure 1). When temperature gradients are steep the region which consists of solid and liquid in the casting is very small. Consequently, liquid metal can be readily transported to the solid-liquid interface to fill the voids caused by solidification contraction. A second potential cause of microporosity, is the precipitation of dissolved gas. The precipitation of gas will occur at the solid-liquid interface as the result of an increase in the gas content of the liquid by rejection of gas from the newly formed solid. If the temperature gradients are steep, and gas content fairly low, the gas rejected from the solid can diffuse from the solid-liquid interface into the remaining liquid, and so even when dissolved gases contribute to microporosity, good directional solidification should minimize this porosity. The interdendritic characteristic of microporosity is shown by a section of a microradiograph taken on a spectroscopic plate and enlarged to 50 diameters (Figure 17). The photographs of Figure 18 also shows this interdendritic characteristic.

Figure 12 is a plot resulting from the extensive survey conducted on the plate castings; it reveals the effect of a chill on the incidence of microporosity. Each of the points on the figure represents the average of data from two to four different microradiographs. The plot of microporosity versus distance is similar for plates with and without a chill. However, the location along the length of the plate at which the level of microporosity becomes quite high is displaced from the end of the plate by the use of a chill. The chill has extended the length of the columnar zone which forms at the end of the plate. In other words, the chill has enhanced directional solidification toward the riser and therefore made adequate feeding of the region near the end of the plate possible.

The plates studied in this series of experiments were apparently free from porosity when examined by conventional radiographic technique; that is to be expected (except possibly for the five inch long, unchilled plate) from published data on feeding distance in steel castings.[29] Nonetheless, by careful microradiographic examination, the presence of microporosity is evident. The effect of the microporosity is presented in Figure 19 which shows a correlation of ductility as measured by the percentage reduction in area in a tensile test and the amount of microporosity. In addition to the data accumulated from the plate castings, data from the other experimental castings are shown on this graph. With very few exceptions, small amounts of microporosity are associated with good ductility, whereas large amounts of microporosity are associated with poor ductility.

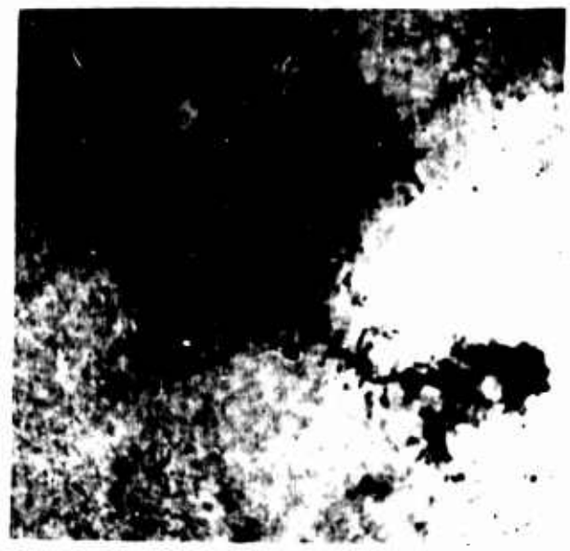

Figure 17 Microradiograph Showing the Interdendritic Nature of Microporosity (50X, porosity is black)

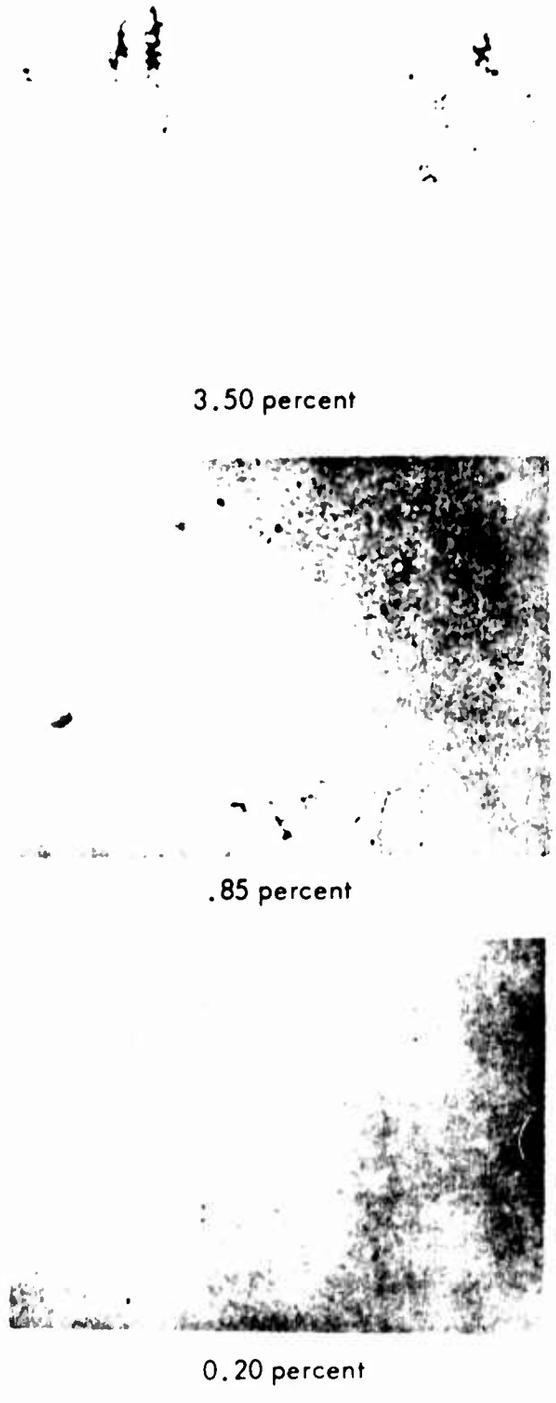

Figure 18 Typical Microradiographs
(approximately 12X, black areas are porosity)

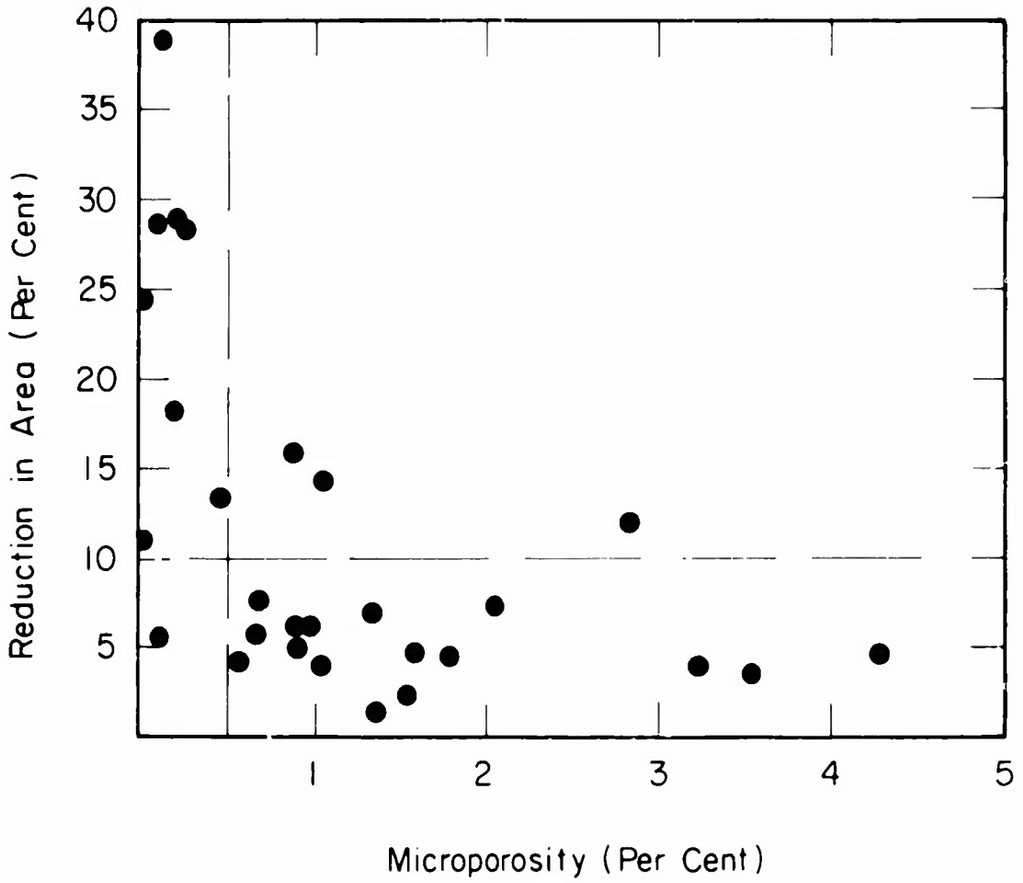

Figure 19 Relationship of Ductility to Microporosity (values taken from all experimental castings)

V. CONCLUSIONS

1. A literature survey is presented which deals primarily with:

   a. Casting structure and its effect on mechanical properties.
   b. Factors affecting formation of columnar zone in steel castings.
   c. Factors affecting formation of equiaxed zone during solidification.

2. A technique for preparing thin samples for microradiographic examination (about .006 inches), was developed and is described. Techniques of radiographing these thin samples to determine the amount of microporosity is discussed. The microradiographic technique was found especially valuable for determining the amount of microporosity in steel castings.

3. A series of cylinder castings was poured to investigate the effect of solidification variables on structure. The presence of a chill on the bottom surface produced a columnar zone and a region relatively free of microporosity. Mechanical properties from the columnar region, as compared with typical properties from cylinder castings were:

Region	Yield Strength lbs/in^2	Tensile Strength lbs/in^2	Elongation Percent	Reduction in area %	Micro-porosity
Columnar Chill Zone (transverse to grains)	218,000	270,000	10.7	27.0	.38
Typical	218,000	272,500	5.0	7.1	1.17

4. A steel rod placed in the riser of a cylinder casting resulted in substantial grain refinement of the equiaxed zone of crystals. Addition of a vibrator did not increase the refinement above that noted with the chill rod alone. Gravity settling of crystals formed in the region near the chill rod appears to be the major grain refining mechanism. No improvement in mechanical properties was detected as a result of the grain refinement achieved.

5. A "denucleation" effect was observed in a casting that was gated by flowing the liquid metal through a vibrating steel box.

6. A series of 1/2" thick plate castings was produced to study the effect plate length and end chilling on microporosity and mechanical properties of the plates. Properties as high as 260,000 psi ultimate tensile strength, 220,000 psi yield strength, and 40 percent reduction in area were obtained near a chill (where microporosity was essentially zero). Microporosity was found to increase (1) if the plate was not chilled, and (2) with increasing distance from the plate end (chilled or unchilled). Mechanical properties, particularly reduction in area and elongation decreased with increasing microporosity.

7. Effects of solidification rate and section size were investigated in step wedge castings. This series of experiments showed that castings could be produced with excellent mechanical properties throughout a two-inch thick section provided steep thermal gradients (good directional solidification) were maintained. By the use of exothermic materials on one surface and a copper chill on the opposite surface, columnar grains were grown throughout a two inch section. A comparison of the mechanical properties of this casting structure with a typical structure in a two inch section solidified in a sand mold is:

Region	Yield Strength lbs/in^2	Tensile Strength lbs/in^2	Elongation Percent	Reduction in area %	Micro-porosity
Columnar chill and exothermic	205,500	268,000	9.3	24.6	.00
Typical sand	205,000	265,000	2.9	7.6	1.60

8. Two heats of castings were prepared by inserting a vibrating prong of steel in the bottom section of a block-like casting. Mechanical properties of the vibrated and unvibrated castings were equal and no change in macrostructure or microstructure was observed However, mechanical properties of both castings were somewhat higher than would be expected in castings of this geometry. It is possible the vibrations were transmitted to the control castings and had a beneficial effect on both castings in each heat.

9. Results of mechanical property tests of material solidified in a flowing stream showed the ductility of the columnar region to be greatly superior to that of the equiaxed region. A comparison of these properties is presented below.

Region	Yield Strength lbs/in^2	Tensile Strength lbs/in^2	Elongation Percent	Reduction in area %	Microporosity Percent
columnar	220,000	288,500	8.6	28.9	27
equiaxed	215,500	224,000	0.7	1.1	1.32

10. A correlation was made between microporosity existing in various locations of all the test castings examined, and the ductility of material from this region. When microporosity level was below .50 percent (this percentage is not a true volume percent but a magnified volume percent determined by the special technique employed), then ductility values of 25 to 28 percent reduction in area can be achieved in this alloy steel heat-treated to a strength level that approaches 300,000 pounds per square inch.

11. A relationship was found to exist between the as-cast structure of steel castings and susceptibility to microporosity; substantially more porosity was found in equiaxed areas of steel castings than in columnar areas. It is shown herein that conditions for the formation of a columnar zone (steep temperature gradients) are identical to the conditions for excellent directional solidification and feeding.

TABLE XIII

Summary of Chemical Analyses

Heat No.	Casting Design	Chemical Element (Percent) C	Mn	Si	Cr	Ni	Mo	P	S
A	Cylinder	.37	.87	.31	.80	1.88	.25	.010	.008
B	"	.40	.82	.40	.85	1.77	.25	.007	.015
C	"	.41	.69	.30	.79	1.91	.24	.008	.012
D	Plate	.38	.72	.32	.87	1.87	.25	.007	.009
E	"	.40	.85	.25	.80	1.81	.26	.013	.008
F	Step Wedge	.40	.99	.31	.97	2.27	.27	.009	.011
G	" "	.40	1.01	.28	.80	2.03	.24	.005	.012
H	Vibration	.37	1.06	.27	.82	1.82	.25	.011	.015
I	"	.37	.91	.26	.81	1.79	.25	.011	.014
J	Flow-out	.43	.84	.33	.83	1.91	.25	.007	.009
	Aim	.40	.80	.30	.80	1.80	.25	--	--

BIBLIOGRAPHY

1. Foundry Section, Metal Processing Division, Department of Metallurgy, Massachusetts Institute of Technology, "Investigation of Solidification of High Strength Steel Castings under Simulated Production Conditions" Final Report, July 1, 1958, Dept. of the Army, Ordnance Corps., Contract Number DA-19-020-505-ORD-4511.

2. Walther, W. D., Adams, C. M., and Taylor, H. F., "Effect of Casting Fiber on Mechanical Properties of Al-4% Cu Alloys", Trans. A. F. S. (1953) 61 p. 664-673.

3. Northcott, H. F., "Mechanical Properties of Metals in the Cast Condition", Institute of Metals (1942) 68 p. 189.

4. Northcott, H. L., "Influence of Turbulence on the Structure and Properties of Steel Ingots". Journal, Iron & Steel Institute (1941) 143, p. 49-88.

5. Reynolds, J. A., and Preece, A., "Metal and Metal Research on Steel Castings, Part I: Solidification Mechanism", Foundry Trade Journal (1955) 99, p. 31-38.

6. Cibula, A., "The Mechanism of Grain Refinement of Sand Casting in Al Alloy", Journal of Institute of Metals (1949-1950) 76 p. 321.

7. Gray, "The Effects of Gravity on the Solidification of Steel", Journal of Iron and Steel Institute (1956) 182 p. 366-374.

8. Hucke, E. E., Flemings, M. C., Adams, C. M., and Taylor, H. F., "Metal Solidification in a Flowing Stream", Trans. AFS (1956) 64, p. 636.

9. Northcott, H. L., "The Influence of Alloying Elements on the Crystallization of Copper", Journal Institute of Metals (1938) 62 p. 101 and (1939) 658 p. 173.

10. Polin, I. V., "Effect of Hydrogen and Nitrogen on Solidification", Steel (1948) p. 55 (See Met. Abs.).

11. Eminger, Z., and Kinsky, F., "Results of Experiments on Vacuum Casting of Steel", Hutnicke Listy 1 (1956)No. 6 p. 25-30, Brutcher Translation No. 3861.

12. Chalmers, B., "Effect of Impurities and Imperfections on Crystal Growth", Impurities and Imperfections A. S. M. (1954) p. 64.

13. Tiller, W. A., and Rutter, J. W., "The Effect of Growth Conditions Upon the Solidification of a Binary Alloy", Canadian Journal of Physics, 34 (1956) p. 96.

14. Walker, J. L., "Structure of Ingots and Castings", Liquid Metals and Solidification, A. S. M. Cleveland (1958) p. 319.

15. Hucke, E. E., Flemings, M. C., Adams, C. M. and Taylor, H. F., "The Degeneration of Freezing Plane Interfaces in a Controlled Solidification System", Internation Symposium on the Physical Chemistry of Process Metallurgy, AIME, Pittsburgh, 1959.

16. Wagner, C., "Theoretical Analysis of Diffusion of Solution During the Solidification of Alloys", Trans. AIME 200 (1954) p. 154.

17. Schiel, E. "Die Entstehung des Gussgefüges homogener Metalle", Zeit. Für Metallkunde 29 (1939) p. 404-409 (Abridged Translation in Metal Treatment (1938) Vol. 4, p. 11-14).

18. Tamman, G., Aggregatzustande 1. Voss, Leipzig (1922) p. 223.

19. Genders, R., "The Interpretation of the Macrostructure of Cast Metals", Journal Institute of Metals (1926) V. 35, p. 259.

20. Freedman, A. H. and Wallace, J. F., "Vibrating Strength into Metals", Modern Castings, V. #1, No. 4, p. 64.

BIBLIOGRAPHY - Contd.

21. Garlick, R. G. and Wallace, J. F. "Grain Refinement of Solidifying Metals by Vibration", Modern Castings, V. 35 No 6 (1959) p. 86-94.

22. Papapetrou, A., "Untersuchungen uber Dendritisches Wachstum von Kristallen" Zeit. Fur Kristallographie V. 92 (1935) p. 89.

23. Trillat, J. J., "Metallurgical Aspects of Microradiography", Met. Reviews 1956, Vol. 1 p. 3-30.

24. Homes and Gouzou, Revue Met. (1951) Vol. 48, p. 251.

25. Engstrom, A. and Lindstrom, B. "The Properties of Fine-Grained Plate Emulsion for Microradiography", Acta Radiologica Vol. 35 (Jan. 1951) p. 33-44.

26. Michael, A. and Bever, M. B., "Solidification of Aluminum Rich Aluminum-Copper Alloys", Trans. AIME Vol. 200, (1954) p. 47.

27. Sharpe, R. S., "The Microradiography of Metals, its Advantages and Limitations" in X-ray Microscopy and Microradiography by Cosslett, U. E., Engstrom A. and Pattee, H. H., Academic Press, (1957) New York 1. 590-602.

28. Jackson, W. S., "Some Features of the Metallurgical Properties of Steel Casting", British Foundryman, April 1957, 50 p. 211-219.

29. Briggs, C. W., "The Solidification of Steel Castings", Steel Founders Society of America, Research Report No. 30, September 1953, Cleveland, Ohio.

30. Gaudin, A. M., Principles of Mineral Dressing, p. 172-183 McGraw-Hill Book Co., New York (1939).

31. Schuhmann, R., Metallurgical Engineering, Addison-Wesley Press, Inc., Cambridge, Mass. (1954).

32. Wulff, J., Taylor, H. F. and Shaler, A. J., Metallurgy for Engineers, J. Wiley & Sons, New York (1952).

APPENDIX

Derivation of Settling Rates of Solid Steel Particles in Liquid Steel

If one considers solid spherical particles of radius r and density, ρ_s, settling as a result of gravity in a liquid of density, ρ_e, whose viscosity is μ, the equation of motion has been given by Newton and Stokes for two cases:

1. Laminar flow:

$$\frac{dv}{dt} = \left(\frac{\rho_s - \rho_e}{\rho_s}\right) g - \frac{9}{2} \frac{\mu}{\rho_s} \frac{v}{r} \tag{1}$$

2. Turbulent flow:

$$\frac{dv}{dt} = \left(\frac{\rho_s - \rho_e}{\rho_s}\right) g - \frac{3}{8} \frac{Q}{\rho_s} \frac{\rho_e V^2}{r} \tag{2}$$

where:

v = the velocity of the particle
t = time
g = gravitation constant (980 cm/sec^2)
Q = resistance factor proportional to the Reynolds Number

If equations 1 and 2 are solved to find the maximum or terminal velocity, v_m, by setting $dv/dt = 0$, then

For the laminar case:

$$v_m = \frac{2}{9} (\rho_s - \rho_e) r^2 g/\mu \tag{3}$$

For the turbulent case:

$$v_m = \sqrt{\frac{8g}{3Q} \left(\frac{\rho_s - \rho_e}{\rho_e}\right) r} \tag{4}$$

Gaudin[30] presents the general solution of equations 1 and 2. The solution for equation 2 is

$$tx = \frac{\rho_s v_m}{2(\rho_s - \rho_e) g} \ln \frac{1 + x}{1 - x} \tag{5}$$

where:

t_x = time to reach a velocity which is a fraction x of the therminal velocity

x = the fraction of the terminal velocity attained = v_x/v_m where v_x is the velocity at time t_x

Equation 5 may be put in a more useful form by use of the identity

$$\tan h^{-1} x = \frac{1}{2} \ln \frac{1 + x}{1 - x} \tag{6}$$

which results in the following equation:

$$x = \frac{v_x}{v_m} = \tan h \left[\left(\frac{\rho_s - \rho_e}{\rho_s} \right) \frac{g t_x}{v_m} \right] \tag{7}$$

which is valid for any spherical particle falling in any medium.

The case for laminar flow may be solved in a similar fashion. This solution yields a slightly more complicated equation. However, no error is introduced by assuming turbulent flow provided that the ratio of time to reach half the terminal velocity to the time to reach the terminal velocity is greater than 0.25. In cases where this ratio is less than 0.25, very small errors are introduced. (See Gaudin, reference 30.)

The distance that a particle falls until it reaches a certain fraction of its terminal velocity can be calculated by integration of equation 1 or 2. Integration of equation 2 with the boundary conditions that the distance is zero at time equal to zero yields:

$$S_x = A v_m \ln \left\{ \frac{2 + e^{t/A} + e^{-t/A}}{4} \right\} = 2 A v_m \ln \left\{ \cosh \frac{t}{2A} \right\} \tag{8}$$

where:

S_x = distance fallen at time t

A = constant equal to $\left(\frac{\rho_s}{\rho_s - \rho_e} \right) \frac{v_m}{g}$

Equation 8 has been solved for the case of the steel by assuming the values given below:

μ = 0.04 poise (from Schuhmann[31])

ρ_e = 7.08 grams cc. } calculated from solidification shrinkage of 3 % given by Wulff, Taylor and Shaler[32]

ρ_s = 7.30 grams cc. }

v_m = 1198 r^2 (calculated from equation 3)

The results of these calculations are plotted in Figure 20 by calculating the distance versus time curve until the particles reach their terminal velocity given by equation 3. At this point, the particles are assumed to move with a constant velocity equal to v_m.

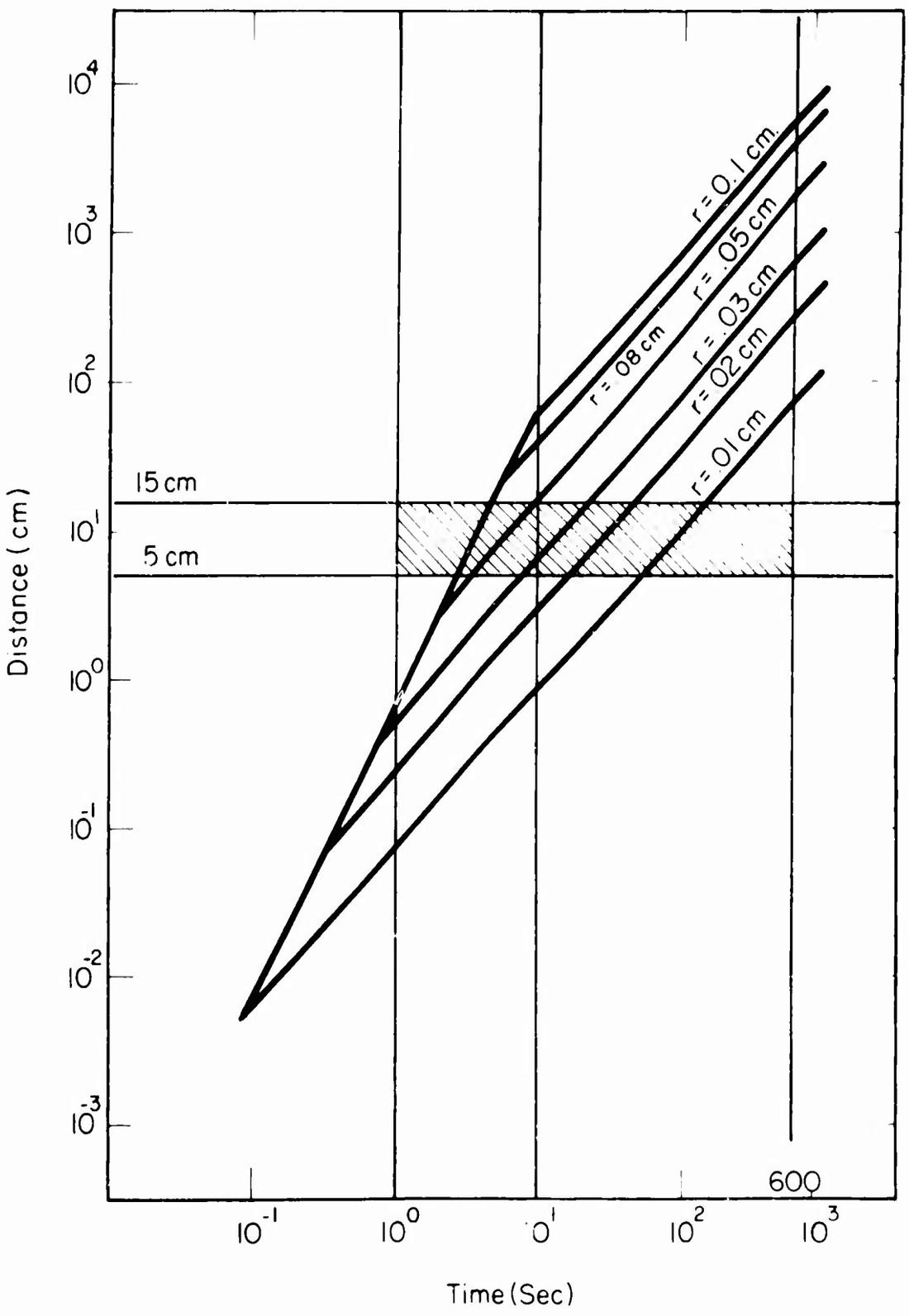

Figure 20 Settling Curves for Steel Particles in Liquid Steel

END